Study of soil carbon dynamics under a bamboo plantation in Belgium

Auteur : Kovacs, Nicolas
Promoteur(s) : Meersmans, Jeroen; Colinet, Gilles
Faculté : Gembloux Agro-Bio Tech (GxABT)
Diplôme : Master en bioingénieur : sciences et technologies de l'environnement, à finalité spécialisée
Année académique : 2021-2022
URI/URL : http://hdl.handle.net/2268.2/15184

Study of soil carbon dynamics under a bamboo plantation in Belgium

NICOLAS KOVACS

Travail de fin d'études présenté en vue de l'obtention du diplôme de master bioingénieur en sciences et technologies de l'environnement

Année académique 2021-2022

Co-promoteurs:
Pr Gilles Colinet
Pr Jeroen Meersmans

Study of soil carbon dynamics under a bamboo plantation in Belgium

NICOLAS KOVACS

Travail de fin d'études présenté en vue de l'obtention du diplôme de master bioingénieur en sciences et technologies de l'environnement

Année académique 2021-2022

Co-promoteurs:
Pr Gilles Colinet
Pr Jeroen Meersmans

Host institutions

This thesis was carried out at the Gembloux Agro-Bio Tech Faculty of the University of Liège, in the Water-Soil-Plants Exchange Department. The external host organisation for the field measurements was the botanical garden "De Kleine Boerderij".

Acknowledgments

First, I would like to express my profound gratitude to Mr Meersmans and Mr Colinet, my two supervisors, for allowing me to work on this subject. Mr Meersmans, for all your explanations and guidance. Saying thank you does not seem enough now that you have helped me complete this journey. I thank you for your remarkably enriching field trips during which I was able to benefit from your experience sharing. Thank you for your patience during our many long meetings, your good mood and your great kindness. Thank you, Mr Colinet, for your precious advice and goodwill, and for allowing me to work in your laboratory.

I would also like to thank Marie Dincher for her valuable advice.

To Stéphane Becquevort for his practical explanations of the probes, availability, and kindness.

To Emilie Marit for her laboratory technical explanations, patience, and good humour.

To Mr Jan Walstra from the Geological Survey of Belgium for his explanations of the geology of Flanders.

To all the staff of Gembloux Agro-Bio Tech, the secretaries and the cooks for their excellent efficiency and good humour.

To my parents for allowing me to pursue a good education, with a special dedication to my father for helping me with my field measurements.

To my lovely girlfriend, Raquel, for being in my life for the past six beautiful years, for her accurate and artistic advice and for motivating me daily.

To Marisol for her thorough proofreading of this document.

To my friends for always being there for me, and my great teammates, without whom this adventure would not have been the same.

Finally, I would like to thank the jury members for agreeing to evaluate me in the context of this work.

To my grandparents

Abstract

Given the increasing concentrations of greenhouse gases in the atmosphere, combating climate change is no longer an option but a necessity. Various methods have been developed, including technologies to reduce greenhouse gas emissions and sequester them. This work falls in the scope of soil carbon sequestration through bamboo planting. A Belgian botanical garden with a bamboo plantation has been used as an experimental field. Multiple samplings were carried out, including soil organic carbon and respiration measurements. The aim was to accurately compare the carbon dynamics between grassland and three bamboo species belonging to the same genus (*Phyllostachys*).

After twelve years of planting bamboo in a grassland, no significant increase in soil organic carbon stock was measured except at a depth of 30 to 40 cm. One species of bamboo emitted less CO_2 from the soil than grassland or the other two bamboo species. Additional experiences, including biomass measurements or chemical analyses, were conducted to justify the findings.

Finally, several improvements to the experimental setup have been proposed. This work opens up multiple perspectives, such as replicating the experiment in a forest or a possible carbon remuneration by policymakers.

Key words: Belgium, bamboo, soil organic carbon, stock, biomass, stability, soil respiration, CO_2 efflux

Résumé

Etant donné l'augmentation des teneurs en gaz à effet de serre dans l'atmosphère, lutter contre le changement climatique n'est plus une option, mais bien une nécessité. Différentes méthodes sont développées, incluant des technologies de réduction des émissions de gas à effet de serre, ou encore celles visant à les séquestrer depuis l'atmosphère. Le présent travail s'inscrit dans le cadre de la séquestration du carbone dans le sol par la plantation du bambou. Un jardin botanique belge possédant des parcelles de bambou a été utilisé en tant que terrain expérimental. De multiples échantillons furent pris, incluant des mesures de carbone organique du sol et de respiration. L'objectif était de comparer fidèlement la dynamique du carbone entre une prairie et trois espèces de bambou appartenant au même genre (*Phyllostachys*).

Après douze ans d'implantation du bambou sur une prairie, aucune augmentation significative du stock de carbone organique du sol n'a été mesurée, à l'exception de la couche de sol entre 30 et $40cm$ de profondeur. Le sol d'une espèce de bambou émettait significativement moins de CO_2 que la prairie ou que les deux autres espèces de bambou. Des expériences supplémentaires, telles que des mesures de biomasse ou des analyses chimiques, ont été mises en place pour tenter de justifier les découvertes.

Finalement, plusieurs améliorations du dispositif expérimental ont été proposées. Le présent travail ouvre la porte à maintes possibilités, telles qu'une reproduction de l'expérience en système forestier ou une éventuelle rémunération carbone par les décideurs politiques.

Mots clés: Belgique, bambou, carbone organique du sol, stock, biomasse, stabilité, respiration du sol, flux de CO_2

Contents

List of Figures

List of Tables

Acronyms

CO_2 Carbon dioxide

CVB   Centrum Voor Bodemkartering

CI   Confidence Interval

CF   Correction Factor

DBH   Diameter at Breast Height

GHG   Greenhouse Gas

CH_4 Methane

OM   Organic Matter

RMI   Royal Meteorological Institute of Belgium

SOC   Soil Organic Carbon

STD   Standard Deviation

SE   Standard Error

TOC   Total Organic Carbon

WRB   World Reference Base for Soil Resources

Chapter 1

Introduction & Literature review

1.1 Context

The current problem of global warming is mainly caused by rising levels of greenhouse gases (GHGs) in the atmosphere, especially the anthropogenic emissions of carbon dioxide (CO_2) and methane (CH_4) (Le Quéré et al., 2015; Yoro and Daramola, 2020). Since the industrial revolution in 1760, the atmospheric carbon dioxide content has increased by 31% (Lal, 2004). This general upward trend is still hastening over time, as shown by the Keeling curve, indicating that the CO_2 concentration has increased from $313 ppm$ in 1958 to $421 ppm$ in June 2022 (UC San Diego, 2022). Human activities, such as burning fossil fuels, industrial processes, conversion of natural ecosystems to conventional agriculture and deforestation, are mainly responsible for these significant increases (Lal, 2004). In particular, deforestation disrupts the carbon cycle, accounting for 25% of the annual GHGs emissions (Al-Ghussain, 2018).

The 26th United Nations Climate Change Conference in Glasgow, more commonly known as the Conference of the Parties (COP26), affirms that further efforts are needed to limit the global average temperature rise to below 2°C. Reducing anthropogenic carbon dioxide emissions by 45% is thus crucial for countries to achieve net zero emissions by 2050 (United Nations, 2021). Many technologies are trying to mitigate climate change, including de-carbonation techniques or industrially absorbing CO_2 from the atmosphere (Panepinto et al., 2021). In addition to these approaches, soil-based greenhouse gas mitigation strategies, such as a change in agricultural practice, are being studied (Chenu et al., 2014; Paustian et al., 2016; Deluz et al., 2020).

A balance between the inputs and outputs of carbon in the system regulates the carbon content of the soil (West and Six, 2007). When this balance allows organic carbon accumulation in the soil, it is called sequestration. However, this process is profoundly complex as it also depends on many environmental variables. The soil organic carbon (SOC) dynamics is rather slow and therefore takes several years to examine and to detect changes (Srivastava et al., 2016). All of this makes it time-consuming to monitor and very laborious to model (Sierra et al., 2012). Despite the difficulties, many studies lead to a better understanding of organic carbon dynamics and sequestration in soils, especially in croplands, grasslands and forests (Chenu et al., 2014; Chenu et al., 2019; Morais et al., 2019). Sequestration of atmospheric carbon in soils in the form of SOC is widely regarded as a promising method for global climate change mitigation (Srivastava et al., 2016). In the long run, combining the reduction of greenhouse gases, CO_2 in particular, from the atmosphere, with better ecosystem management seems achievable.

1.2 Carbon dynamics

As the scope of this work focuses on soil carbon dynamics, a review of the mechanism of atmospheric carbon storage in soil is made. Soils worldwide are a vital compartment for carbon sequestration (Lal, 2013). Ontl and Schulte, 2012, define soil carbon sequestration as *"a process in which CO_2 is removed from the atmosphere and stored in the soil carbon pool"*. Chenu et al., 2019, recommend differentiating between sequestration and storage, as the latter refers to a SOC stock increase. Between 1500 and 2400 Pg (peta gram = 10^{15}g) of organic carbon is stored in the first two metres of soil. In comparison, about three to four times less carbon is present in vegetation (450 to 650 PgC) and three times less in the atmosphere (830 PgC) (Chenu et al., 2014; Paustian et al., 2016; Bispo et al., 2017; Tiefenbacher et al., 2021).
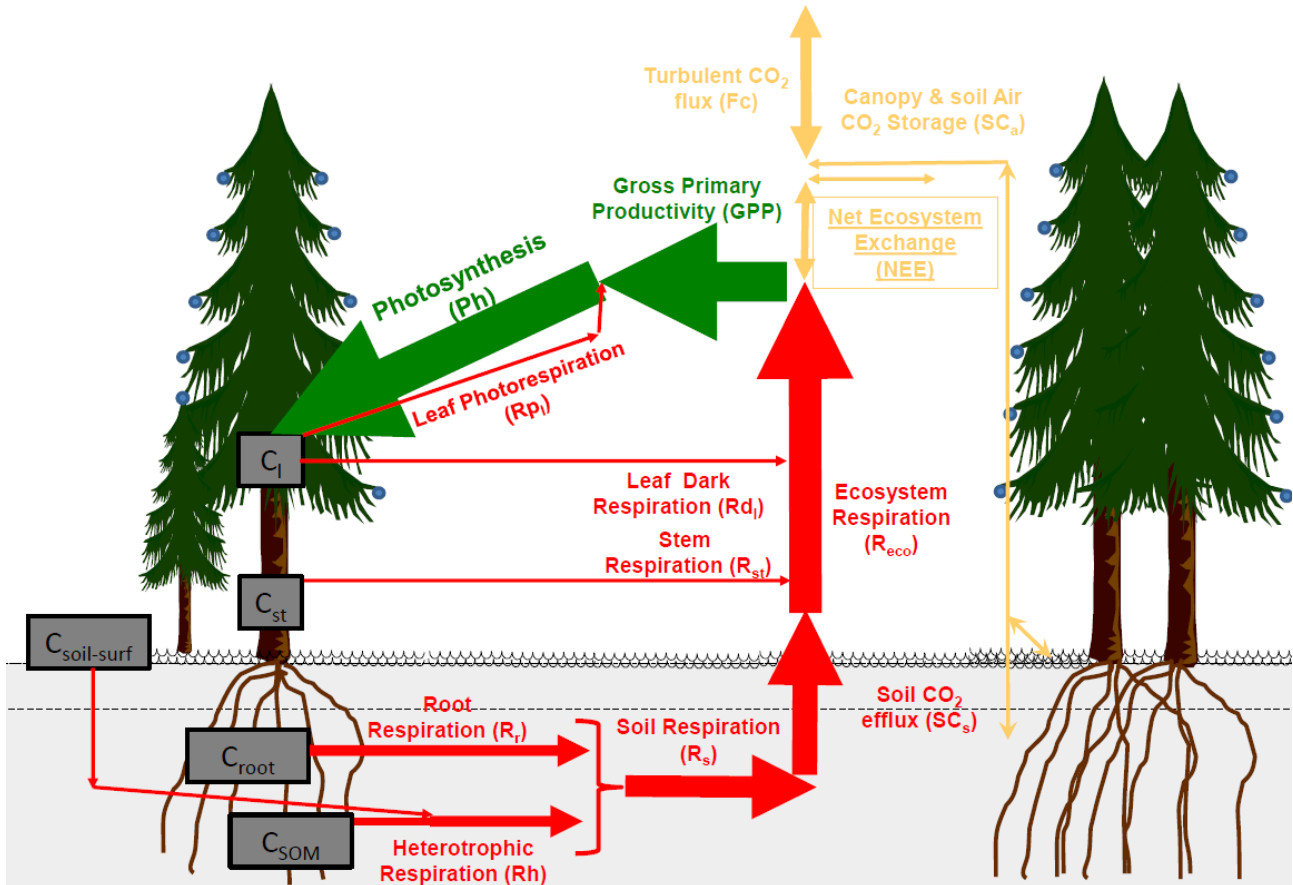
Figure 1.1: Carbon cycle in a terrestrial ecosystem (Longdoz, 2021)

Soil carbon sequestration occurs mainly through plant photosynthesis, also known as Gross Primary Production (GPP), after which the carbon is stored in the soil as soil organic carbon (SOC) (Ontl and Schulte, 2012) (Figure 1.1). The Net Ecosystem Exchange represents the exchange of CO_2 efflux between the air and the terrestrial ecosystem. It is therefore equal to the sum of Gross Primary Production and ecosystem respiration (Yuan et al., 2011). The latter includes all CO_2 effluxes that leave the ecosystem to the atmosphere, and is often simplified to soil respiration. Finally, soil respiration represents the sum of the autotrophic respiration of the living roots and the heterotrophic respiration of the organic matter that decomposes under the action of microorganisms (Ngao et al., 2007). In other words, soil respiration encompasses the functioning of CO_2-producing plant cells and the respiration of microorganisms.

Different environmental variables influence respiration and photosynthesis effluxes. Firstly, ecosystem respiration increases with rising temperatures (Melillo et al., 2002; Yuan et al., 2011). The water content of the soil can also affect respiration. Indeed, when the soil is dry, microorganisms have more difficulty accessing dissolved organic carbon (DOC), thus resulting in lower respiration (Yang et al., 2019). The last parameter influencing respiration is the R_{10} factor, also known as basal respiration rate (Z. Zhou et al., 2013). It is a system-specific factor that depends on the amount of biomass. It represents the respiration of the ecosystem when it is at 10°C.

The factor that most affects Gross Primary production is the Photosynthetic Photon Flux Density (PPFD). It corresponds to the number of photons in the visible range of radiation (400 to $700nm$), reaching the plant per square metre per second [$\mu mol\ m^{-2}\ s^{-1}$] (Ritchie, 2010). The higher this variable, the higher the photosynthesis, considering a saturation level. The last variable that strongly influences the inflow of CO_2 into the plant is the Vapour Pressure Deficit (VPD), defined as the difference between the actual air pressure and the vapour pressure in the leaf. When this difference is too significant, the leaf stomata close, leading to a decrease in photosynthesis (McAdam and Brodribb, 2015).

Many drivers influence the storage of SOC. Firstly, climate, whose temperature directly affects mineralisation, and thus humidity accelerates the weathering of the parent mineral, resulting in the formation of SOC-stabilising mineral surfaces (Wiesmeier et al., 2019). The vegetation type and land use are crucial parameters in SOC storage (Viscarra Rossel et al., 2014). Thus, there will be less carbon input to an agricultural field, the soil organic matter (SOM) protective aggregates are more degraded, and the plot is also more often subject to erosion (Wiesmeier et al., 2019). The second point is very important in the stabilisation of the SOM. Soil aggregates can be divided into macroaggregates ($250-2000\mu m$) and microaggregates ($53-250\mu m$) (Six et al., 2000; Six et al., 2002). A conventional agricultural system under tillage decreases the formation of SOM-protecting micro-aggregates. Conversely, a no-till farming system will reduce the macroaggregates turnover, leading to SOM-stabilising microaggregates (Six et al., 2000).

Six et al., 2002, identifie three mechanisms for stabilising SOM: physical protection by microaggregates, which has just been presented, chemical protection and biochemical protection. Chemical protection consists of an association via chemical links between the SOM and the clay or silt particles. The biochemical protection corresponds to the SOM's chemical composition, whose complexity makes its degradation more difficult in the soil. However, this last point has been much debated for the past years (Schmidt et al., 2011). Lehmann and Kleber, 2015, propose that the biodegradability of SOM in the soil depends on the interactions with aggregates and the metallic links between SOM and soil minerals. A modern view of thermodynamics suggests that the chemical SOM composition does not control its biodegradability in soil. In litter, however, this conclusion does not apply, and the chemical complexity of SOM delays its degradation.

Finally, the multiple benefits of soil carbon storage should not be overlooked. It increases soil fertility, thus implying better agricultural productivity, it acts as a soil cement and helps combat erosion, it contributes to climate regulation when the soil is well managed, and it also serves as a carbon source for connected aquatic environments (Meersmans et al., 2008; Lehmann and Kleber, 2015). Now that the carbon dynamics basics have been presented, the case of bamboo can be investigated.

1.3 Presentation and morphology of bamboo

The term bamboo refers to the subfamily Bambusoideae. It is a grass family (Poaceae) member and is the only grass lineage to have completely diversified and developed in forests (Liese and Köhl, 2015; Saarela et al., 2018). Its taxonomic classification has evolved considerably towards the end of the 20th century, thanks to advances in molecular biology (Zhang et al., 2020). Nearly 1500 species of bamboo have been recorded in Asia, America and Africa. The latitude range for bamboo is 47°S to 50°N, and they can be found between sea level and 4300 metres above sea level (Liese and Köhl, 2015). Bamboo has been used for artistic and technological purposes for centuries (Liese and Köhl, 2015). It is also part of the daily life of some populations who use it to build houses, monuments, or even supply water (Humanitarian, 2009; Mirmehdi, 2016).

The aerial stem of bamboo, called the culm, is a vertical, circular, hollow extension (Figure 1.2a) (Liese and Köhl, 2015). Some culms can be up to 30 metres high and 30 centimetres wide (Rocky and Thompson, 2018). The branches are usually inserted at the nodes. The root system of the bamboo is highly developed. Underground, a rhizome initiates the development of a whole network of roots that join together to connect several culms (Figure 1.2b) (Liese and Köhl, 2015; Rocky and Thompson, 2018). The roots can reach great depths, depending on the species and age of the plant.

(a)   (b)
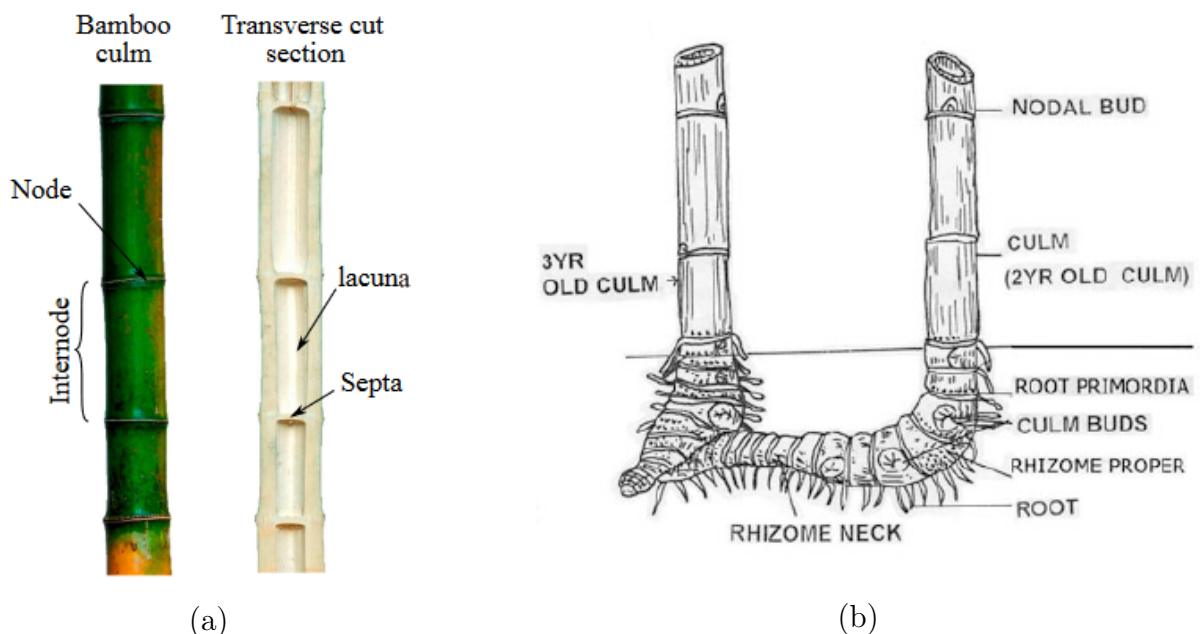
Figure 1.2: Morphology of bamboo with (a) the above ground culm (Gangwar and Schillinger, 2019) and (b) the below ground part of the plant, showing a typical rhizome (Liese and Köhl, 2015)

Bamboo grows remarkably fast. It can sometimes grow up to $100-250cm$ per day (Rocky and Thompson, 2018; Basak et al., 2021). Its mechanical properties are being increasingly studied. It has good tensile strength, is relatively light and does not require replanting thanks to its well-developed root system (Humanitarian, 2009; Samson and Adeniyi, 2015; Rocky and Thompson, 2018; Sanchez et al., 2019). In addition, the bamboo culms from six months to three years old can be harvested to extract their fibres. Compared to cotton planting, ten times more fibre per unit area can be obtained from bamboo (Rocky and Thompson, 2018).

1.4 Bamboo as a carbon sequestration strategy

Bamboo forests cover a considerable part of Asian regions (Chen et al., 2009). For example, bamboo occupies approximately 4.99 million hectares of China's territory. Its large extent underlines the importance of knowing the SOC stock of bamboo. Chen et al., 2009, quantifie the carbon content of the aerial part of a China's Moso bamboo forest at 20.85 $[Mg\ ha^{-1}]$. The SOC stock, 71% of which is stored in the first $40cm$, depends on the type of forest management, i.e. extensive or intensive. The extensive management respects the natural conditions of the forest ecosystem as much as possible, while avoiding human disturbance. It is more effective in storing organic carbon in the soil than intensive management (Chen et al., 2009). The latter involves removing all the grasses from the vegetation cover while adding fertilisers. The authors also showed the growth of carbon stock in bamboo in the past decades, and predicted the same trend for the future with the expansion of bamboo forests.

Li et al., 2015, also worked on the same Chinese forest. Using several databases, they show that the bamboo forest will continue to play a crucial role in the future as a carbon sink. They also argue that tree selection is paramount in the models. This step should optimise the economic and ecological potential of bamboo. Finally, the authors highlight the excellent properties of bamboo as a building material. The industry is sustainable, and bamboo products become a long-term carbon sink (Li et al., 2015).

More recently, Lin et al., 2018, studied SOC's chemical composition eleven years after converting a natural bamboo forest to intensive management. The results show that this conversion significantly decreases SOC contents and stocks in the first $40cm$ of the profile. By studying carbon stability through cumulative CO_2 efflux expressed in $[mgC\ kg^{-1}]$, they show that this conversion improved carbon stability. The decrease in SOC mineralisation is notably linked to the decline in labile carbon content. However, when looking at the net carbon balance, the improved stability is counterbalanced by the stock diminution (Lin et al., 2018).

Soil bulk density is another factor that can be linearly correlated with SOC content. As the former increases, the latter will often decrease (Minasny et al., 2006). This linear trend is valid regardless of the depth of the soil layer considered. However, this correlation is statistically stronger in the first $30cm$ of soil (Tsui et al., 2013). It can be explained by increased organic matter content and lower clay content. Finally, according to Tsui et al., 2013, and their study in the Taiwan mountains, SOC stocks are also positively correlated with the type of vegetation and the Taiwanese mountainous landscape's altitude.

Since the aerial parts, i.e. mainly the culms, also play a role in carbon sequestration, allometric equations are developed to model the sequestered content as a function of various measurable bamboo parameters (Henry et al., 2013).

Yuen et al., 2017, report a rigorous comparison between several bamboo forests and temperate evergreen forests. By synthesising the data, they can quantify the total carbon content of the ecosystem. This value includes the carbon contained in the above-ground parts, i.e. the trunks and leaves, the below-ground parts, i.e. the roots mainly, and the organic carbon in the soil. They show that soil organic carbon accounts for 76% of the total carbon in the bamboo ecosystem, and 74% of the total carbon in evergreen forests (Yuen et al., 2017). In addition, the bamboo forest has an excellent potential to sequester atmospheric CO_2 compared to other terrestrial ecosystems (G. Zhou et al., 2011).

Finally, the effect of depth on the SOC stock of bamboo is also demonstrated. Collecting data from more than 52 separate Asian sites shows a trend of increasing SOC stock with depth (Yuen et al., 2017). It highlights the importance of considering the lower horizons when calculating SOC storage. The policymakers' role is underlined as it is up to them to take pro-carbon storage decisions in the light of scientific advances.

1.5   Main problem & objectives of the study

Scientific studies on the SOC storage of bamboo have gained importance in recent years. However, these studies are mainly limited to quantifying the stock at a specific time or modelling its evolution. Few studies make a rigorous comparison between the transition from an ecosystem to a bamboo plantation.

The present work, therefore, aims to:

(i) Compare SOC stock between grassland and three bamboo species planted on the same land 12 years ago. The intra-bamboo variability must also be studied, and explanations for the possible variations should be considered.

(ii) Compare the soil CO_2 efflux between these four vegetation types. These analyses also aim to determine the stability of the SOC. Explanations for possible variations must also be considered.

Chapter 2

Material & Methods

2.1 Study site description

2.1.1 History

The study site is located in Merksplas, a small municipality on the northern side of Belgium. The experiment took place in the botanical garden De Kleine Boerderij. The region has a unique history. It started in 1822 when the Dutch government founded the Colony of Merksplas (Figure 2.1a). Belgium did not yet exist, and the territory still belonged to the Kingdom of the Netherlands. Low-income families used to live on small, separate farms, each with a plot of land to cultivate. It was an agricultural solution to the growing problem of beggars.

After the Belgian independence in 1830, the project evolved. Beggars by birth, ended up in Wortel, a nearby municipality. People who begged due to debauchery were locked up in Merksplas (Gevangenismuseum, n.d.). Shortly after the First World War, a penal agricultural school was founded. The agricultural work occurred on the small farm, translated in Dutch as "de kleine boerderij". The Colony came to an end in 1993 with the abolition of the vagrant law (Plantentuin Merksplas, 2022). Jan Oprins, a plant collector and current botanical garden owner, acquired 8 hectares of land. He turned it into an educational centre called De Kleine Boerderij, where visitors can attend guided tours.

(a)   (b)
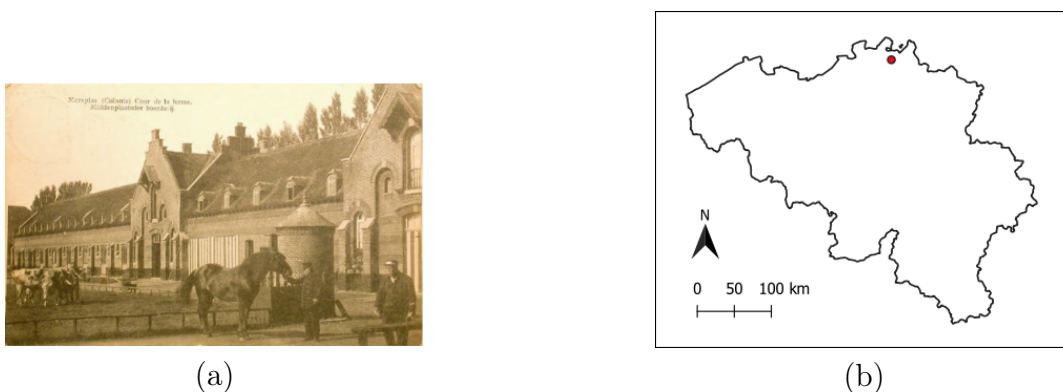
Figure 2.1: Colony of Merksplas with (a) the old Farmyard (Gevangenismuseum, n.d.) and (b) the map of Belgium where the red dot highlights Merksplas

2.1.2 Climate

The study site (51°20'53"N, 4°49'38"E) is located in northern Belgium (Figure 2.1b) and has a temperate climate. From data collected by the Royal Meteorological Institute of Belgium (RMI) between 1991 and 2020, the average temperature over the year in Merksplas is 10.8°C, and the average annual precipitation is 893.5 mm. The average maximum temperature (23.6°C) occurs in summer, which runs from June to September, while the average minimum temperature (0.8°C) occurs in winter, which runs from December to March.

2.1.3 Geology

The mapping area is part of the Antwerp Kempen, also called Northern Kempen. Since the system under study concerns the upper soil horizons, it is necessary to look at the Quaternary geology. The Quaternary map shows the most superficial, and therefore the most recent, geological layers, i.e. deposits of the last 2.58 million years. The thickness of the Quaternary deposits varies within the Antwerp mapping area from 60 metres in the northern part to less than 10 metres in the southern part (Bogemans, 2005). The surface layer is mainly formed by sand deposited by the wind during the Last Glacial Period, known as the Weichselien. Dutch literature commonly calls that aeolian sand *dekzand*. The Quaternary geology is composed of successive deposits on top of each other. According to their composition, geologists have classified them into 42 types (Bogemans, 2005; Databank Ondergrond Vlaanderen, 2020), as illustrated in Figure 2.2.
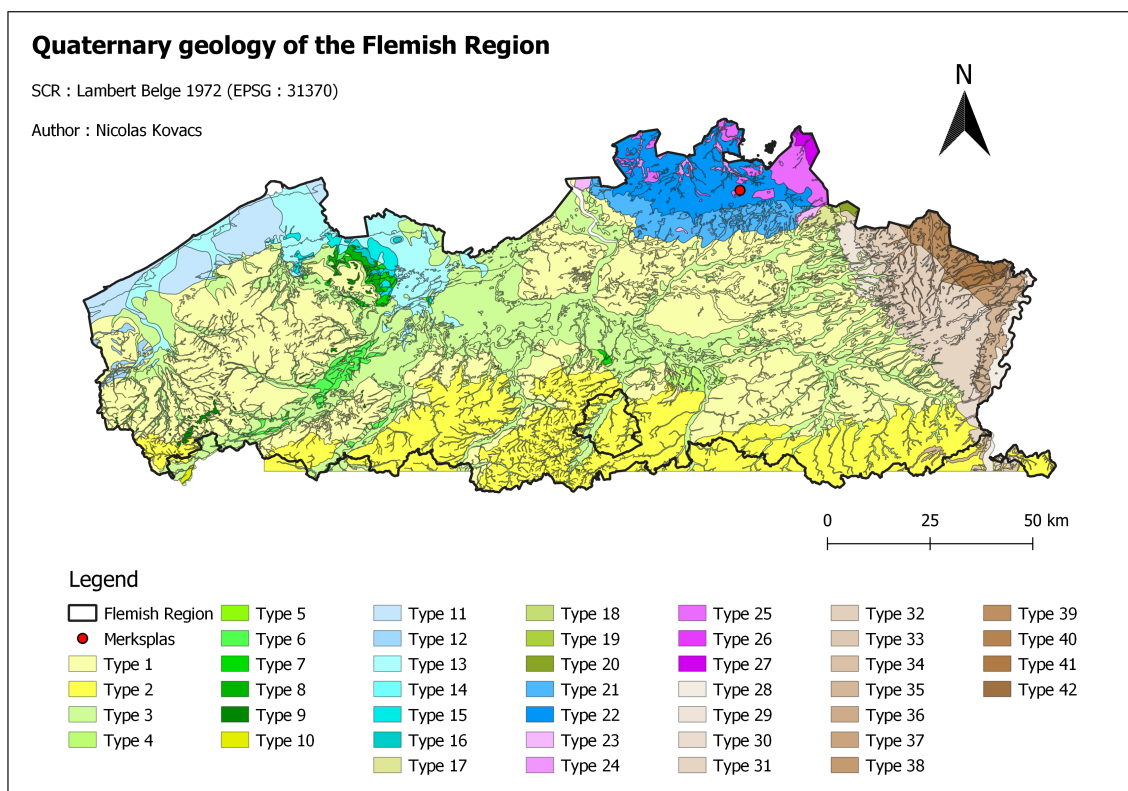
Figure 2.2: Quaternary map of the Flemish Region where the red dot highlights Merskplas

The map's purpose, however, is only to give a first overview of the spatial distribution of geological types within the Flemish Region. This map is a generalisation based on smaller original maps at a scale of 1:50,000. Since the study area is relatively small, looking at the local map for the geological type is essential.

8
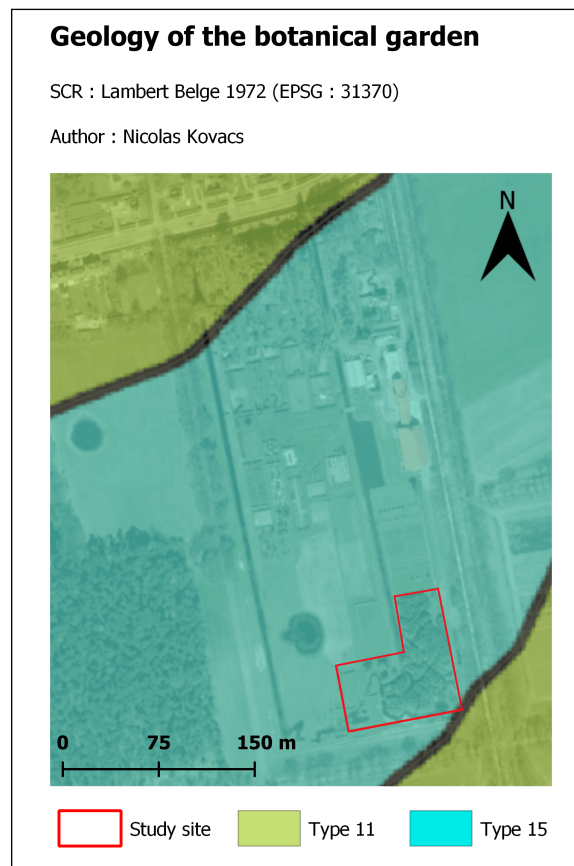
Figure 2.3: Quaternary map of the botanical garden "De Kleijne Boerderij" where the red area highlights the study site. The legend is based on the detailed map initially made at a 1:50,000 scale. Background image: Orthophoto 2022

Figure 2.3 shows the underlying Quaternary geology of the botanical garden "De Kleine Boerderij", where the experiments took place. The map reveals that the study site belongs to type 15 and is surrounded by type 11. Each geological type is characterised by its lithostratigraphy, which consists of several successive sedimentary layers. Figure 2.4 shows the type 15 lithostratigraphy in a two-dimensional sequence from top to bottom.
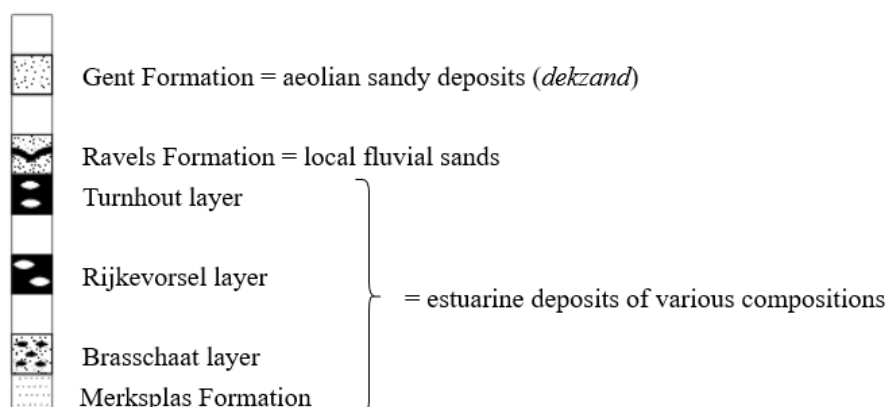
Figure 2.4: Lithostratigraphy of type 15 (adapted from Databank Ondergrond Vlaanderen, 2020). *The lithostratigraphy of type 11 is the same as type 15 without the Ravels Formation*

9

The Gent Formation corresponds to the surface layer and dates from the Late Pleistocene. Its thickness varies and can be up to 2 or 3 metres deep (Bogemans, 2005). The Ravels Formation, which dates from the Early Pleistocene, is underneath and can be up to 3 metres deep; in some places, it comes very close to the surface, merging with it. In the context of this work, the geology of the soil studied corresponds to eolian sandy deposits, which may be mixed with local fluvial sand deposits.

2.1.4 Pedology

The cartographic unit used to characterise soils is the series developed by the Centrum Voor Bodemkartering (CVB) (Van Ranst and Sys, 2000). Each soil series is represented by a three-letter code, which refers to the three main characteristics of the soil profile: soil type or texture, drainage and profile development or horizon succession. The digital soil type map of the Flemish Region (Databank Ondergrond Vlaanderen, 2017) indicates that the study site, which was highlighted in red in Figure 2.3, lies on a *Zcg* soil. The meaning of each letter is given in Table 2.1. In order to verify the information of the digital map, a soil core, which was augered from the study site, is shown in Figure 2.5.

Table 2.1: Soil description of the study site according to the digital map of Flanders

Letter	Characteristic	Meaning
Z	Texture	Sand
c	Drainage	Moderately dry soil
g	Profile development	Humus/iron B horizon (Podzol)
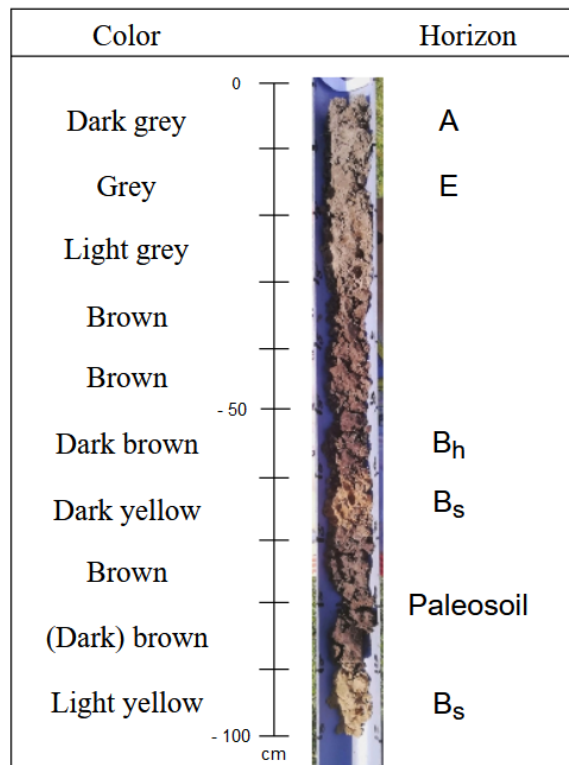
Figure 2.5: Soil profile description of the grassland from the study site. *Each colour corresponds to a 10cm section. The colours are only based on a personal visual interpretation*

Following the identification method of the World Reference Base for Soil Resources (WRB), Figure 2.5 indicates the presence of a diagnostic horizon called the *spodic horizon*, located between 50 and 60cm depth. It is defined as a "*dark colored subsurface horizon with illuvial amorphous substances composed of organic matter and aluminum, with or without iron*" (Singer, 2008). This definition corresponds to the visual observation on-site, thus naming this humus horizon as a Bh. The soil profile analysis, therefore, fits well with the podzol indicated by the digital map.

The pedogenesis of the site can now be explained. An eluvial E horizon was bleached by organic acids that complex aluminium (Al) and iron (Fe), commonly known as acidocomplexolysis (Mokma et al., 2004). The soluble metal-organic complex was therefore transported to the lower horizons. This migration is called cheluviation. Its accumulation in the underlying horizon forms the black B_h spodic horizon, rich in organic matter and typical of podzol. Two factors are required for this vertical transfer of the soluble metal-organic complex. Firstly, some precipitation is needed. This parameter appears to be present as the average annual rainfall is 893.5mm. The physical (particle mobilisation) or chemical (organic acids production) character of this downward migration of Al, Fe, and dissolved organic matter (DOM) is notably linked to high and low percolation, respectively (Krettek and Rennert, 2021). The second requirement is an initially highly siliceous parent material, such as a sandy material or a quartzite loaded with silica and, therefore, quartz (Soil Atlas of Europe, 2005). The study area also meets this second criterion. Finally, the yellow colour indicates the presence of mineral elements. The yellowish illuvial horizon Bs is an accumulation horizon of iron and aluminium oxides.

What happens at a depth of 70cm and below is specific to the region. A new brown horizon lies below the first Bs horizon. An observation of a quarry located 940 metres southeast of the study site has been carried out to discover the origin of this horizon. Figure 2.6 reveals a darker horizon at a depth of 2 metres. This horizon slopes upwards towards the surface, towards the north, i.e. coming up to the study site. It could therefore be found at a depth of 80cm at the study site.
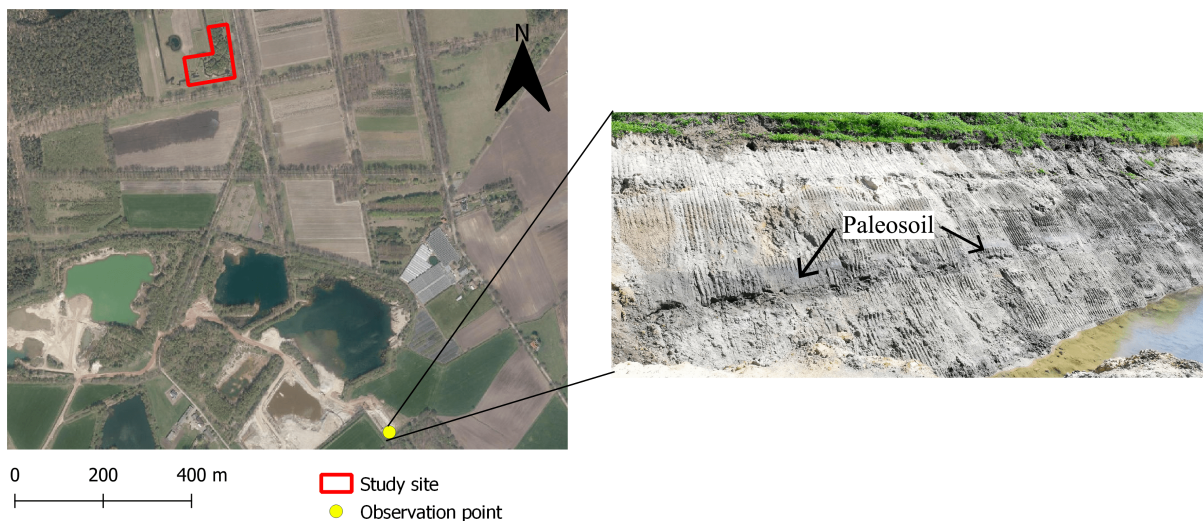
Figure 2.6: Geographical location of the paleosoil. The yellow dot highlights the location (51°20'59"N, 4°49'59"E) from which the photo (right) was taken and thus the position of the palaeosoil. Background image of the map: Orthophoto 2022. *Source: personal photo (right)*

Furthermore, an ice age took place before the beginning of the Early Pleistocene. Glacial erosion is likely to have occurred, and a paleosoil may have set afterwards, i.e. at the beginning of the Early Pleistocene. The Early Pleistocene climate was warm, very wet, and consisted mainly of an interglacial period. The land was heavily impacted by marine and river water. Sea and river deposits (gravel, sand and clay) occurred on a large scale. It also contributed to the development of lush vegetation, enriching the soil with organic matter (Wesselingh and van den Hoek, n.d.). The Early Pleistocene led to the Ravels Formation. The latter typically contains paleosoils with rich organic matter, sometimes even peaty horizons [1]. It reinforces the hypothesis of a paleosoil, on which the podzol described above would have developed.

2.2 Equipment

2.2.1 Soil sampling

A typical auger has collected all soil samples (Figure 2.7a). Lines were drawn in black every $10cm$ to take the same soil depth. A root auger has taken undisturbed soil samples with a constant and known volume (Figure 2.7b). Knowing the volume allowed us to calculate bulk densities and root masses.

(a)

(b)

Figure 2.7: Soil sampling equipment with (a) the auger and (b) the root auger. *Source: Eijkelkamp*

2.2.2 Soil respiration

A portable CO_2 gas analyser (EGM-5, PP Systems) (Figure 2.8a) was used to monitor the CO_2 efflux out of the soil. It is a lightweight instrument (1.5 kg) with a 7.2V battery that allows 16 hours of autonomy. The analyser is easily transportable and therefore very convenient to use. A soil respiration chamber (SRC-2, PP Systems) (Figure 2.8b) connected the gas to the analyser. It is made of PVC and has a circular metallic end that can combine with a white collar (PP Systems). The combination provides good air sealing. It is essential because the wind is more potent when making on-site measurements and could bias the measures. Some authors recommend differentiating soil respiration from CO_2 efflux for short-term measurements because a small part remains trapped in the soil porosity (Maier et al., 2011). However, the measured CO_2 efflux will be referred to as soil respiration for ease of understanding.

---

[1]This information has been confirmed by Mr Jan Walstra, a geologist at the Geological Survey of Belgium.

(a)   (b)

Figure 2.8: Soil respiration measuring equipment with (a) the EGM-5 Portable CO_2 Gas Analyzer and (b) the SRC-2 Soil Respiration Chamber. *Source: PP Systems*

The analyser, already calibrated by the manufacturer, works as follows. Mid-infrared light is sent through a cell. When a target gas, i.e. a CO_2 molecule, enters the cell, it absorbs some infrared energy. A sensor can then measure the decrease in infrared energy at the other end of the cell (2.9). The Beer-Lambert attenuation law states that the infrared signal received by the detector decreases with increasing target gas concentration. The infrared absorption spectrum of CO_2 is at 4.26 μm. Because there is limited overlap with other molecule's absorption bands, that wavelength offers acceptable accuracy. The analyser finally measures a molar concentration in [$ppm\ CO_2$], i.e. [$\mu mol\ CO_2\ \mu mol^{-1}\ air$].
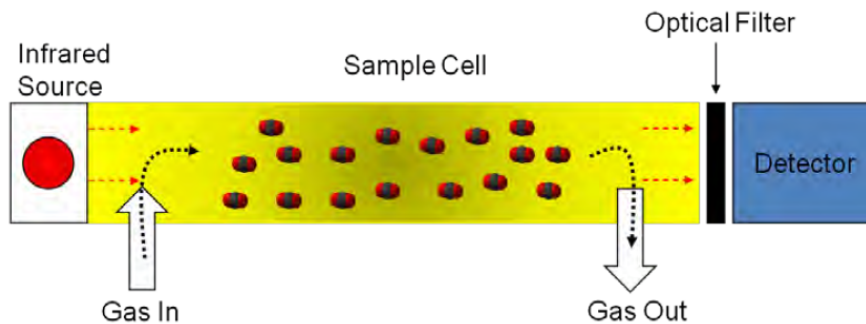
Figure 2.9: Schematic of the gas analyser operation (EGM-5 datasheet). *Source: PP Systems*

Since CO_2 efflux depends on environmental variables, a sensor (5TM, Decagon Devices) (Figure 2.10a) connected to an electronic reader (ProCheck, Decagon Devices) (Figure 2.10b) was used to measure soil temperature and water content. Each temperature and moisture measurement was made simultaneously as the soil respiration measurement.

(a)   (b)

Figure 2.10: Soil temperature and water content measuring equipment with (a) the temperature and humidity sensor and (b) the electronic reader. *Source: Decagon Devices*

The 5TM sensor was chosen because it is compact and allows instant measurement at the desired location. The electronic reader (ProCheck) automatically outputs the soil temperature [°C] but not the water content. The latter is monitored by the 5TM probe using capacitance technology to calculate the dielectric constant ε_r [-], also known as relative dielectric permittivity. The dielectric constant is the ability of a material, i.e. the soil, to store electrical charge (Meter Group, n.d.). By creating an oscillating wave of 70Mhz frequency, the sensor sends an electromagnetic field in the surrounding medium (5TM datasheet). The soil's dielectric permittivity will impact the wave's amplitude and the electromagnetic field's charge (Shaikh et al., 2019). Because the soil particles' moisture and spatial arrangement influence the dielectric constant, the new charge determines the soil water content (Capparelli et al., 2018). The raw signal given by the sensor and read by the electronic reader must finally be divided by 50 to obtain the dielectric constant ε_r.

The 5TM sensor was calibrated on sandy soil (4.8% clay, 3.8% silt, 91.4% sand) from Ten Aard and stored by the Soil Physics and Mechanics Laboratory of Gembloux Agro-Bio Tech[2]. The scientific literature calibrates this type of probe based on the known volumetric water content $[cm^3\ cm^{-3}]$. However, this parameter could not be calculated as the bulk density of the calibrated soil was unknown. For this reason, the gravimetric water content w [%] (equation 2.1) was used instead. It is not detrimental to the measurement campaign as the soil moisture was used as a proxy for soil respiration and not to make a detailed hydrodynamic study of the soil. Figure 2.11 shows the gravimetric water content calibration curve of the 5TM sensor. Though the fit is often polynomial (Kim et al., 2008; Shaikh et al., 2019), the low permittivity range is usually linear (Cobos, n.d.).

$$w\ [\%] = \frac{\text{Weight of wet soil } [g] \text{ - Weight of dry soil } [g]}{\text{Weight of dry soil } [g]} \times 100 \qquad (2.1)$$
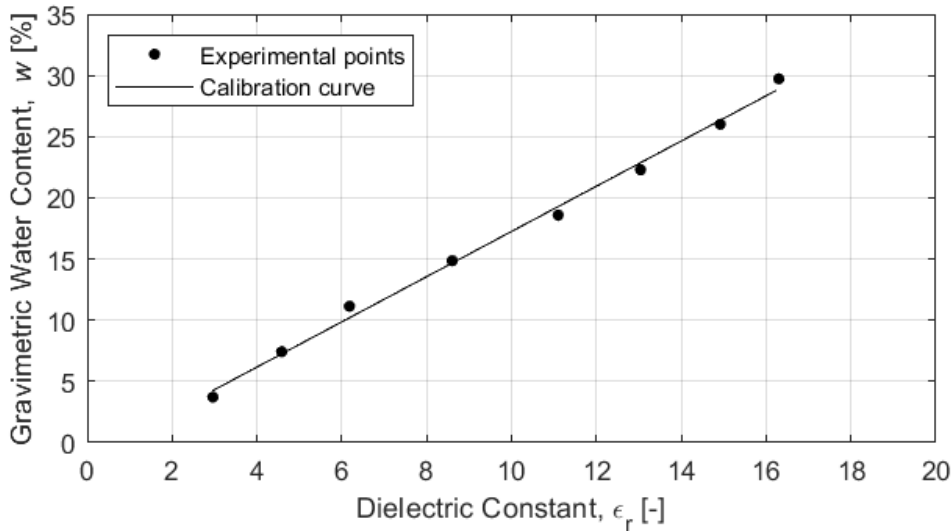
Figure 2.11: Gravimetric water content calibration curve
$$w = 1.8467 \times \varepsilon_r - 1.2118$$
$$R^2 = 0.995$$

---

[2]It would have been preferable to calibrate the probe on soil from the study site. However, to be representative, this step requires a significant quantity of soil to be sampled. The experiments also aimed to avoid destroying the vegetation typed for guided tours for the public. A soil of the same particle size was therefore considered acceptable.

14

2.2.3   Soil organic carbon analysis

Two techniques were used to quantify the organic carbon content of the soil $[gC\ kg^{-1}]$: the dry combustion method and the Walkley & Black chemical method.

Dry conbustion

The agricultural soil testing laboratory of La Hulpe conducted soil organic carbon (SOC) analyses by dry combustion. This method uses an analyser that heats the soil to a very high temperature. All the carbon is then oxidised to carbon dioxide, which an infrared detector can measure. The method finally provides a content expressed in $[gC\ kg^{-1}]$.

Walkley & Black

The Walkley & Black method measures easily oxidisable carbon by chemical titration. It was carried out in the Water-Soil-Plant Exchange laboratory of Gembloux Agro-Bio Tech. The assay[3] is based on the oxidation of organic carbon by potassium dichromate ($K_2Cr_2O_7$) in a strongly acidic medium (H_2SO_4). Reducing Cr^{6+} to Cr^{3+} releases oxygen used to oxidise the organic carbon. This oxidation is an exothermic reaction that is not accelerated by heating in the Walkley & Black method. Equation 2.2 represents the overall oxidation reaction.

$$\begin{cases} 2\ K_2Cr_2O_7 + 8\ H_2SO_4 \longrightarrow 2\ K_2SO_4 + 2\ Cr_2(SO_4)_3 + 8\ H_2O + 3\ O_2 \\ 3\ C + 3\ O_2 \longrightarrow 3\ CO_2 \end{cases} \tag{2.2}$$
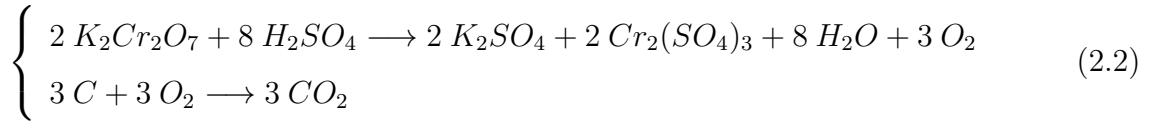
Mohr's salt $[Fe(NH_4)_2(SO_4)_2.6H_2O]$, a reducing agent, titrates the excess oxidant in the presence of a colour indicator called diphenylamine. NaF is also added to complex the Fe^{3+} ions formed. This last step aims to prevent a redox reaction between these ions and the colour indicator. The titration is completed when the colour changes from violet to dark green. Equation 2.3 gives the titration reaction.

$$K_2Cr_2O_7 + 6\ Fe(NH_4)_2(SO_4)_2 + 7\ H_2SO_4 \longleftrightarrow Cr_2(SO_4)_3 +$$
$$7\ H_2O + 6\ Fe(NH_4)(SO_4)_2 + K_2SO_4 + 3\ (NH_4)_2(SO_4) \tag{2.3}$$
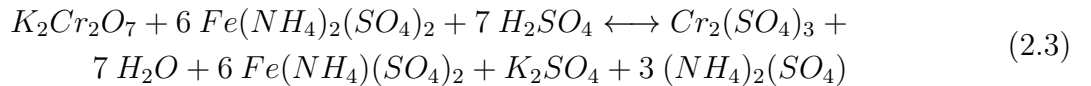
Finally, the organic carbon content of the soil is calculated by equation 2.4. The factor 10 converts a content expressed in $[\%]$ to $[\%_{oo}]$, i.e. $[gC\ kg^{-1}]$.

$$SOC[gC\ kg^{-1}] = 10 \times (x - x') \times C_{Mohr} \times 0.3 \times m^{-1} \tag{2.4}$$

x and x' are the volume $[ml]$ of titration solution (Mohr's salt) used for the blank and soil sample titration, respectively. C_{Mohr} is the Mohr's salt concentration $[mol\ l^{-1}]$, 0.3 is the factor corresponding to the mgC oxidised per reaction (De Vos et al., 2007) and m is mass of the soil sample $[g]$. Equation 2.4 does not take into account the correction factor (CF).

---

[3]The complete protocol is available from the Water-Soil-Plant Exchange laboratory.

2.3 Methodology & Sampling

2.3.1 Plot selection

The main ideas were to compare soil organic carbon dynamics between grassland and bamboo, and the variability between several bamboo species as well. First, a grassland and a bamboo plantation with the same soil type (Zcg) were selected based on the digital soil map of Flanders. This initial need allowed us to define a provisional study perimeter. The soil type needed to be the same, as soil's texture, drainage, and groundwater rise influence the carbon dynamics (Meersmans et al., 2007).

The agricultural history also had to be identical, as different practices lead to distinct vertical distributions and long-term carbon storage in the soil (Virto et al., 2012; Chenu et al., 2019). This information was checked on Geopunt, the central access point to geographical government information. No agricultural vegetation type change (grassland) was observed between 1979[4] and 2010 when the bamboo was planted. This last criterion strongly restricted the first perimeter. The final study site is shown in Figure 2.12. It includes grassland and bamboo, all on the same soil type (Zcg) and with the same agricultural history. Since the bamboo was planted on this grassland, comparing their soil organic carbon dynamics is justified and accurate.
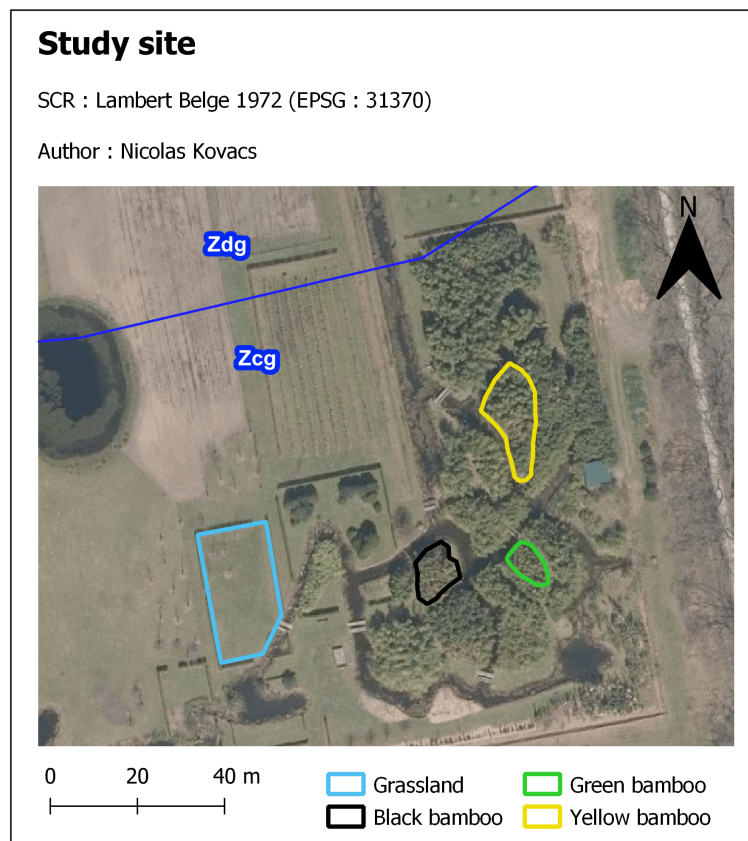

Figure 2.12: Description of the study site, including a grassland and three bamboo species. Soil type Zcg corresponds to the study area. The nearby Zdg soil type corresponds to moderately wet soil and is marked out by the dark blue line. Background image of the map: Orthophoto 2022

---

[4]Geopunt does not give any images prior to this date.

Once the study site had been delimited, three bamboo species belonging to the same genus (*Phyllostachys*) were selected: black bamboo (*Phyllostachys nigra*), green bamboo (*Phyllostachys aurea*) and yellow bamboo (*Phyllostachys aureosulcata*), as illustrated by Figure 2.12. The selection was made based on the colour of the trunks, the species, and the accessibility of the plots. Some bamboo plots were too dense to go in and were therefore eliminated. The choice of three bamboo plots was based on a balance between a sufficient number of species to compare while avoiding a massive number of samples to analyse. In addition, the yellow bamboo had bigger culms, which would be interesting to compare with the other bamboo plots. Table 2.2 shows some characteristics of the four plots studied and aims to visualise the study site well. A square of 9 m^2 was delineated to count the bamboo culms. The square surrounded the soil respiration measurement area and included the augered samples. Counting the number of culms revealed their density within the large square.

Table 2.2: First description of the four plots studied. *The density of the culms is based on a square of 9 m^2 representative of the plot.*

Plot	Plot area [m^2]	Culm density [$Culms\ m^{-2}$]
Grassland	445.22	/
Black bamboo	93.06	19
Green bamboo	57.15	15
Yellow bamboo	199.54	9

The square was also used to measure the average culm diameter. As reported in the literature, a digital caliper measured the diameter of the culms at breast height (DBH), i.e. $1.3m$ high (Fu et al., 2014; Prayogo et al., 2021). These diameter measurements were then used to calculate a soil occupancy rate for bamboo (equation 2.5), which indicates what percentage of the soil is occupied by bamboo culms. This factor was calculated to explain potential variations in soil organic carbon stock.

$$\text{Occupancy } [\%] = \text{Average culm area } [m^2] \times \text{Culm density } [Culms\ m^{-2}] \times 100 \qquad (2.5)$$

Finally, a 50-cm square was constructed to collect the leaves on the ground. Three bags of leaves were collected per bamboo plot in order to try to explain the possible variation in soil organic carbon stock.

2.3.2 First exploration of the system

First, an initial prospecting was conducted to know the system better. The first three soil cores per plot were taken using an auger, with a $50cm$ distance between them. It was decided to take samples in $10cm$ layers up to a depth of 1 metre. The objective of this prospecting was to visually analyse the twelve soil profiles on-site and to observe how deep the roots went. It revealed differences between the horizons, especially with depth. For this reason, the samples were all analysed independently rather than as composites. Each $10cm$ layer was then dried at 40°C, crushed and sieved to $2mm$, and finally sent to the testing laboratory of La Hulpe for total carbon (organic + inorganic) analysis of the 120 samples. As none of the samples contained inorganic carbon, soil organic carbon (SOC) is referred to as total organic carbon (TOC) [$gC\ kg^{-1}$].

The statistical analysis of this first system exploration was carried out as follows. The depth of each plot contains three replicates (n = 3). The depths of two separate plots (e.g. grassland vs black bamboo) were compared one by one by calculating the standard error (SE) (equation 2.7). The standard error is the ratio between the standard deviation (STD) (equation 2.6) and the square root of the number of samples. While the standard deviation gives an idea of the measurement uncertainty, the standard error gives an idea of the uncertainty of the model used. In this case, the model in question was the total SOC mean $\tilde{y}$ (n = 3).

$$STD = \sqrt{\frac{\sum_{i=1}^{n}(y_i - \tilde{y})^2}{n-1}} \qquad (2.6)$$

$$SE = \frac{STD}{\sqrt{n}} \qquad (2.7)$$

Next, a confidence interval (CI) per depth was calculated using the standard error. A normal distribution of carbon content values was assumed because it is impossible to check normality on only three samples. It was not detrimental to the analysis as this step was only a first exploration of the system. Equation 2.8 shows the confidence interval formula with a 95% level of confidence. Finally, a double comparison had to be made. For the same depth, if the first plot's (e.g. grassland $0-10cm$) mean ($\tilde{y}_1$) falls outside the second plot's (e.g. black bamboo $0-10cm$) confidence interval (CI_2), and if the second plot's mean ($\tilde{y}_2$) falls outside the first plot's confidence interval (CI_1), then the two means are significantly different (equation 2.9). If at least one mean falls within the confidence interval of the other, the two means are not significantly different.

$$CI = [\tilde{y} - 1.96\ SE;\ \tilde{y} + 1.96\ SE] \qquad (2.8)$$

$$\text{if}\ \tilde{y}_1 \notin CI_2\ \textbf{and}\ \text{if}\ \tilde{y}_2 \notin CI_1 \longrightarrow Sig. \neq \qquad (2.9)$$

This double operation was carried out by comparing each depth of the grassland, from $0-10cm$ to $90-100cm$, with black bamboo, green bamboo and yellow bamboo. Intra-bamboo comparisons were not made at this stage as it was only a first prospecting of the system.

2.3.3   Further investigation

The first exploration of the system limited the depth of interest. Figures 3.1, 3.2 and 3.3 (see chapter "Results & Discussion") concluded that the actual depth of interest was between 0 and $40cm$. For this reason, the second part of the results will only focus on a more statistically robust comparison of the plots between 0 and $40cm$ in depth.

Therefore, a second soil sampling was carried out, focusing on the $0-40cm$ depth. Each plot sampled seven other locations: four with the auger and three with the root auger, with a minimum distance of $1m$. For each new sampling point, four depths were sampled: $0-10cm$, $10-20cm$, $20-30cm$ and $30-40cm$. In total, 4 depths $\times$ 4 cores (auger) $\times$ 3 cores (root auger) $\times$ 4 plots = 112 new samples were collected. Each $10cm$ layer was then dried at 40°C, crushed and sieved to $2mm$. The testing laboratory of La Hulpe then analysed the SOC content $[gC\ kg^{-1}]$ by dry combustion. The samples taken with the root auger were also used to calculate soil bulk density $[kg\ m^{-3}]$ and root mass $[g]$ for each of the four depths (n = 3). Root masses were weighed as a proxy for carbon inputs.

These samplings made the comparison of the four depths between each plot possible, each depth containing ten replicates (n = 10). As the SOC stocks showed non-normality distribution (Shapiro-Wilk test, $p < 0.05$), a Kruskal-Wallis test was performed for each of the four depths to test the influence of vegetation type, i.e. the qualitative variable. The continuous quantitative variable was the SOC stock for each $10cm$ layer, also called SOC mass by surface unit $[kgC\ m^{-2}]$, calculated using equation 2.10 (Meersmans et al., 2011). The null hypothesis (H_0) then states that the means of the SOC stocks of each plot are equal. The transition from content to stock was crucial since the work aimed to quantify organic carbon storage in the soil. It was, therefore, necessary to take into account the bulk density of the soil.

$$\text{SOC}_{\text{mass}} = \rho_s \times \frac{SOC}{1000} \times d \tag{2.10}$$

Where SOC_{mass} is the soil organic carbon stock per surface unit $[kgC\ m^{-2}]$, ρ_s is the average soil bulk density $[kg\ m^{-3}]$ (n = 3 for each depth), SOC is the soil organic carbon content measured by dry combustion $[gC\ kg^{-1}]$ and d is the the soil sampling depth ($= 0.1m$). In order to perform a multiple pairwise comparison between the four plots, a Dunn $post-hoc$ test was carried out. It compared SOC stocks between the grassland and the three bamboo species, and studied the intra-bamboo variability as well.

Finally, an analysis of organic carbon by the chemical method of Walkley & Black was conducted. This approach has a significant drawback. It does not consider the recalcitrant fraction of organic carbon, leading to an underestimating of the overall SOC content and necessitates using a correction factor (CF) (De Vos et al., 2007; Lettens et al., 2007; Meersmans et al., 2009). The present study, however, benefited from this limitation by deliberately wanting to know the recalcitrant part of the organic carbon. Organic carbon analysis was therefore carried out on every sample taken during the prospecting of the system, analysing only from 0 to $40cm$ as this was the actual depth of interest. The idea was then to see if the growth of the bamboo since 2010 has been able to bring a protection for soil's organic carbon.

Typically, the SOC contents obtained by dry combustion and the Walkley & Black method are compared by performing a linear regression without intercept, i.e. passing through the origin (Meersmans et al., 2009). However, this methodology requires a considerable number of samples. The present approach only contained three replicates per depth and plot. The results were quantified by calculating the correction factor (CF) of each sample, equal to the ratio between the dry combustion SOC content and the Walkley & Black SOC content. A one-way ANOVA (Shapiro-Wilk, $p > 0.05$; Levene, $p > 0.05$) on the CF according to the vegetation type was performed. Then, a two-way ANOVA was carried out to test a possible effect of depth.

2.3.4 Soil respiration measurement

For each plot, three white collars were installed in the soil (Figure 2.13), leaving a volume of $339cm^3$ outside the ground[5]. The number of three was chosen to replicate measures and to study the intra-site variability of CO_2 efflux. Within each collar, grass and leaves were removed so that their respiration was not considered (Rodtassana et al., 2021). In this way, the total respiration of the soil could be measured, i.e. the autotrophic respiration of the living roots and the heterotrophic respiration of the organic matter that decomposes under the action of microorganisms (Ngao et al., 2007).

---

[5]This information is necessary as this volume had to be manually encoded in the system (EGM-5) to be added to the initial volume of the respiration chamber (SRC-2).
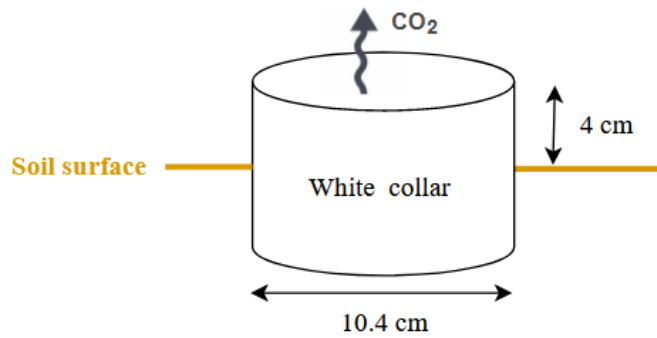
Figure 2.13: Position of the white collar in the soil to which the respiration chamber (SRC-2) is attached. *Source: personal drawing*

The first CO_2 efflux measurement started two weeks after installing the white collars to allow the system to stabilise. Soil respiration measurements were conducted over six days, leaving at least two weeks between each measurement day. Each data collection was carried out in the following way. A one-minute delay was considered after the chamber was placed on the ground to establish stable gradients before the start of measurements. The EGM-5 analyser monitored a concentration increase $[ppm\ CO_2]$ for seven minutes. A CO_2 efflux $[ppm\ CO_2\ s^{-1}]$ was obtained by dividing the concentration increase by the measurement time. First, this step was repeated three times on each white collar in order to study the variability within the same emission source, i.e. the white collar. As each plot contained three white collars, nine CO_2 efflux were monitored each day for each plot. On each measuring day, the order of the measured plots changed and was randomly selected to avoid a bias in the measurements.

In addition to the CO_2 efflux, soil water content and temperature were recorded beside the white collars. A minimum of three measurements were made on each plot. Figure 2.14 illustrates the experimental setup on-site. The white rings of the grassland were relatively close to each other as the plot is still used for guided tours and mowed. However, the distances between each white collar of the three bamboo plots were more considerable ($0.5-1m$).
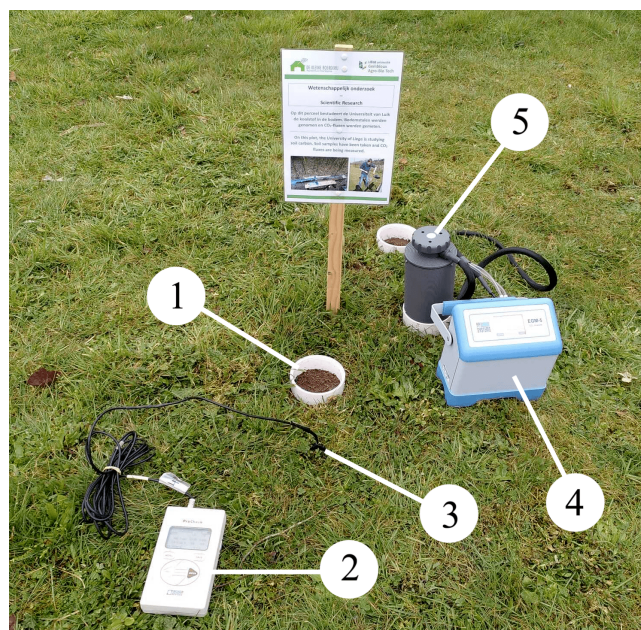
Figure 2.14: Soil respiration setup with **1**: white collar; **2**: ProCheck; **3**: 5TM Soil Moisture and Temperature Sensor; **4**: EGM-5 Portable CO_2 Gas Analyser; **5**: SRC-2 Soil Respiration Chamber

Two units were used to express the soil respiration results: $[\mu mol\ CO_2\ m^{-2}\ s^{-1}]$, which is a raw measure, and $[mgC_{respired}\ g_{soil}^{-1}\ hr^{-1}]$, which is a relative measure whose purpose is to take into account the stability of soil organic carbon.

Using equation 2.11, the recorded CO_2 efflux $[ppm\ s^{-1}]$ was converted to $[\mu mol\ m^{-2}\ s^{-1}]$ as this is a unit widely used in the scientific literature (Longdoz et al., 2000). This equation was provided in the datasheet of the EGM-5 analyser.

$$F_s\ [\mu mol\ m^{-2}s^{-1}] = \frac{dC}{dt} \times \frac{P}{1013} \times \frac{273.15}{T_{air}} \times \frac{1}{22.414} \times \frac{V}{A} \times 10^3 \qquad (2.11)$$

Where F_s and dC/dt both represent the measured CO_2 efflux from the soil, respectively expressed in $[\mu mol\ m^{-2}\ s^{-1}]$ and $[ppm\ s^{-1}]$. P is the barometric pressure $[mbar]$, T_{air} is the air temperature [°K], 22.414 is the Ideal Gas constant at standard pressure and temperature $[L\ mol^{-1}]$, V is the volume of the system $[m^3]$, A is the soil area $[m^2]$ and 10^3 is the last conversion factor $[L\ m^{-3}]$. The normality of CO_2 effluxes was first checked (Shapiro-Wilk test, $p > 0.05$). The variances, however, were sometimes not homogeneous (Levene test, $p < 0.05$). It was probably because some values came from the same white collar. As a result, either one-way Welch's ANOVA (Levene test, $p < 0.05$) or one-way ANOVA (Levene test, $p > 0.05$) test was performed, each day, to test the influence of the vegetation type, i.e. the qualitative variable. The null hypothesis (H_0) then stated that the means of the CO_2 effluxes of each plot are equal. In order to perform a detailed multiple pairwise comparison between the four plots, a Games-Howell post$-$hoc test was carried out. It compared CO_2 effluxes between the grassland and the three bamboo species, and studied the intra-bamboo variability as well.

Apart from this first conversion, the raw CO_2 efflux $[ppm\ s^{-1}]$ was also converted to $[mgC_{respired}\ g_{soil}^{-1}\ hr^{-1}]$. This unit provided a relative measure of the soil organic carbon stock. Since the latter is respired and goes from the soil to the atmosphere, it was of paramount importance to measure the carbon's stability with respect to its respiratory character. Equation 2.12 was taken from the datasheet for converting $[ppm\ s^{-1}]$ to $[g\ CO_2\ m^{-2}\ hr^{-1}]$ and was then modified according to the literature to obtain the flux relative to the SOC stock $[mgC_{respired}\ g_{soil}^{-1}\ hr^{-1}]$ (equation 2.13).

$$F_s\ [gCO_2\ m^{-2}hr^{-1}] = \frac{dC}{dt} \times \frac{P}{1013} \times \frac{273.15}{T_{air}} \times \frac{44.009}{22.414} \times \frac{V}{A} \times \frac{10^3}{10^6} \times 3600 \qquad (2.12)$$

$$F_s\ [mgC\ g^{-1}hr^{-1}] = \text{equation } 2.12 \times A \times \frac{12}{44} \times 10^3 \times (SOC_{mass} \times A)^{-1} \qquad (2.13)$$

Where dC/dt represents the measured CO_2 efflux from the soil $[ppm\ s^{-1}]$, 44.009 is the molar mass of CO_2 $[g\ mol^{-1}]$, 10^3 (2.12) is a conversion factor $[L\ m^{-3}]$, 10^6 (2.12) is another conversion factor $[\mu mol\ mol^{-1}]$, 3600 changes from seconds to hours $[s\ hr^{-1}]$, 12/44 is the ratio of the atomic mass of C to that of CO_2, 10^3 (2.13) changes from g to mg, SOC_{mass} is the SOC stock recalculated to the depth of the white collar in the ground $[g\ m^{-2}]$. An ANOVA test on relative effluxes was then performed in the same way.

Finally, two Analysis of Covariance (ANCOVA) tests on the relative effluxes were performed. The ANCOVA was used to compare the means of relative CO_2 effluxes between several plots, also taking into account the link between the efflux and a covariate, i.e. soil temperature or water content.

2.3.5 Methodology diagram

Figure 2.15 summarises the main analyses carried out in this work.
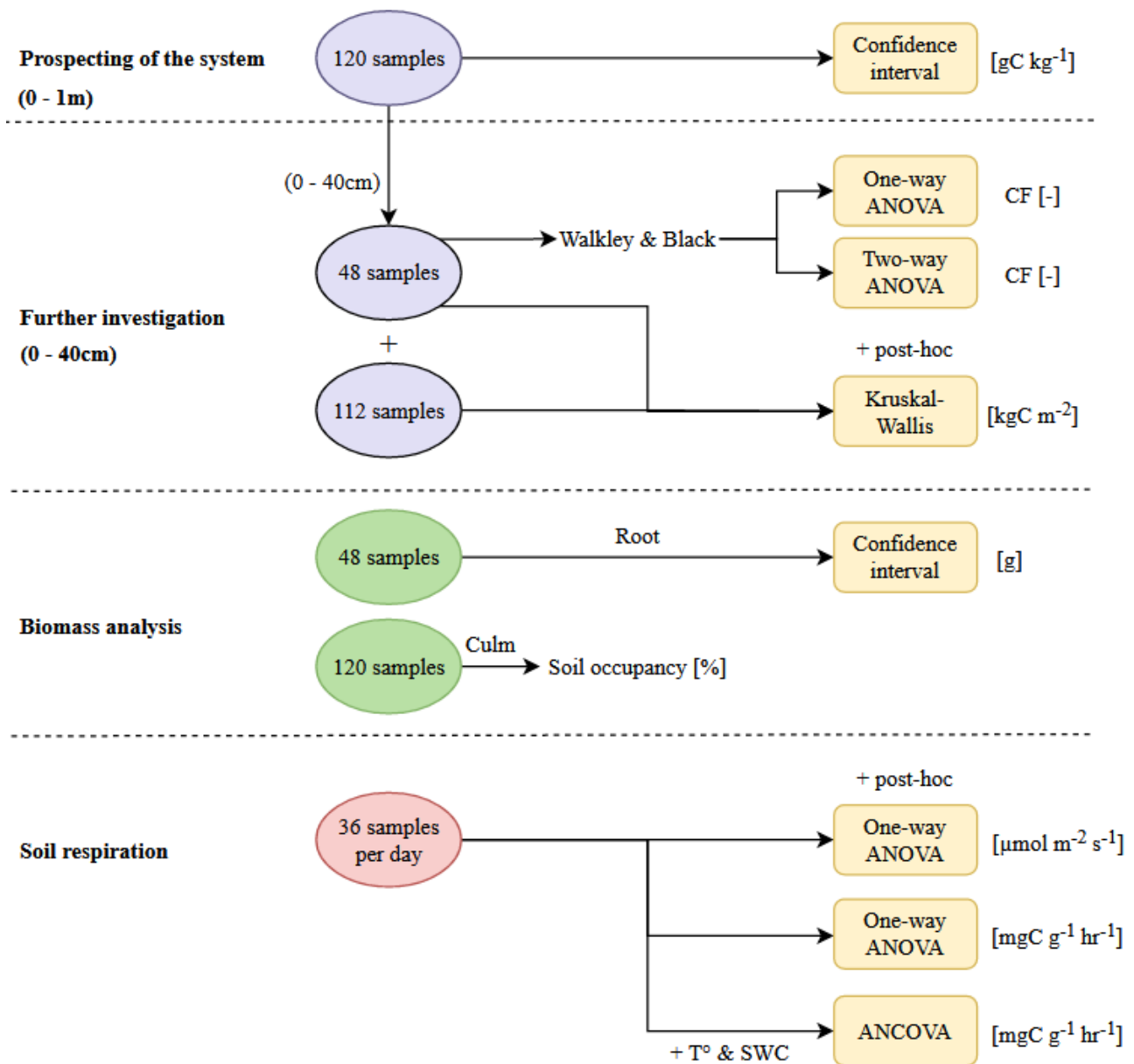
Figure 2.15: Summary of the main steps and analyses

2.3.6 Software

Statistical analyses were performed using Rstudio 2022.07.1 software, while graphs were constructed on Matlab R2018a.

Chapter 3

Results & Discussion

3.1   First exploration of the system

Figure 3.1: Comparison of the vertical distributions of SOC $[gC\ kg^{-1}]$ (mean ± standard deviation, n = 3) between the grassland and the black bamboo. The contents were obtained by dry combustion. Code (assuming a normal distribution): No symbol $p > 0.1$, • $p < 0.1$ (90% conf. level), ∗ $p < 0.05$ (95% conf. level),   ∗∗ $p < 0.01$ (99% conf. level), ∗ ∗ ∗ $p < 0.001$

Figure 3.1 shows the evolution of the vertical distribution of organic carbon $[gC\ kg^{-1}]$ between the surface and 1-metre depth. The values in the graph can be visually correlated to the individual soil profiles at the same level. As an overall trend, organic carbon decreases non-linearly to $50-60cm$ depth before increasing again to $80-90cm$ depth. This trend can be observed in both the grassland and the black bamboo.

The surface horizon A, which is generally a mixture of organic matter and minerals, is hardly observable in the grassland's soil profiles. It contrasts sharply with a forest podzol where the A horizon is very black with small white spots.

23

The decline over the first grassland horizons is in line with theory. Some models have already demonstrated the non-linearity of carbon decrease with depth (Meersmans et al., 2008). The drainage class influences the slope of this curve, as does the soil texture. Furthermore, sandy soils have large pore sizes and therefore have high permeability. On the other hand, clay soils have much smaller pore sizes and, therefore, generally have low permeability. Thus, vertical transfers of dissolved organic carbon by infiltration and leaching might occur more efficiently in sandy soil. The organic matter-rich spodic horizon is easily observable in the photos of the grassland profiles, whereas it is less so in those of the black bamboo. The reason is that the photos of the black bamboo were taken in the shade. However, this spodic horizon, typical of Podzols, is more easily detected by looking at the individual distributions of each profile (Appendix B). The SOC contents in Figure 3.1 include standard deviations, which also complicates this diagnostic horizon's observation.

The vertical distribution of carbon resembles a decreasing exponential in the grassland, thus reflecting the site's history, which has always been occupied by grassland. It would have been alarming finding a constant carbon content over the first 30 cm of the profile, as this would have indicated a conventional agricultural past (Meersmans et al., 2008). This non-linear decrease over the first 30 to 40 centimetres coincides with the satellite images since 1979 (Geopunt Vlaanderen, 2022).

Figure 3.1 shows a significant difference ($p <$ significance level) between the SOC values of grassland and black bamboo at $0-10cm$ and $60-100cm$ depth. The standard deviations (SD) indicate measurement uncertainty, while the $p - value$, considering the standard error (SE) and the confidence interval (CI), indicates an error in the calculated mean. Though the two standard deviations overlap at $70-80cm$ depth, a significant difference ($p < 0.05$) is still present.

Figure 3.2 shows that almost all SOC differences between grassland and green bamboo are significant beyond $20cm$ depth. However, this is because the soil profiles of green bamboo are remarkably different. The first and third soil columns do not appear to represent a podzol, but rather a podzolic cambisol as no illuvial yellowish horizon Bs is detectable. It means there is either less acidity or less infiltration, and podzol formation is slowed down.

Figure 3.3 shows that almost all SOC differences between grassland and green yellow bamboo are significant between the surface and $70cm$.

Another interesting point is that the deep organic carbon re-increase is always lower in-depth than on the surface. It would tend to confirm the hypothesis that the paleosoil dates from the Pleistocene, and the old carbon it contains has been degraded over time. Moreover, the supposed paleosoil position is closer to the surface in the yellow bamboo than in the rest of the plots. It would again tend to confirm the paleosoil hypothesis, as the paleosoil rose towards the surface in a northerly direction, and the yellow bamboo is the northernmost plot.

Nevertheless, another intriguing aspect persists. The bamboo profiles have very dark horizons. The black colour indicates a potent, complex and often poorly accessible presence of organic matter (OM). It could theoretically come from an ancient charcoal production area, where the usable carbon would have degraded. In order to verify this new hypothesis, a sample was analysed using a magnifying glass with Mr Colinet. The coal has a theoretical shiny surface and appearance, which was not observed here.
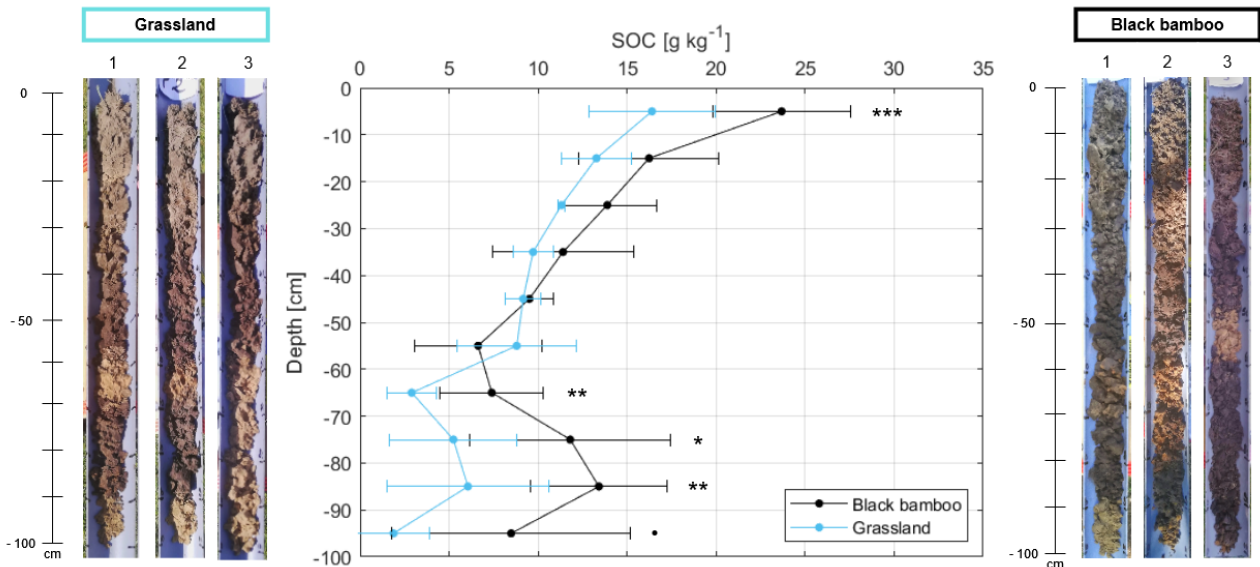
Figure 3.2: Comparison of the vertical distributions of SOC $[gC \ kg^{-1}]$ (mean $\pm$ standard deviation, n = 3) between the grassland and the green bamboo. The contents were obtained by dry combustion. Code (assuming a normal distribution): No symbol $p > 0.1$, $\bullet$ $p < 0.1$ (90% conf. level), $*$ $p < 0.05$ (95% conf. level), $**$ $p < 0.01$ (99% conf. level), $***$ $p < 0.001$
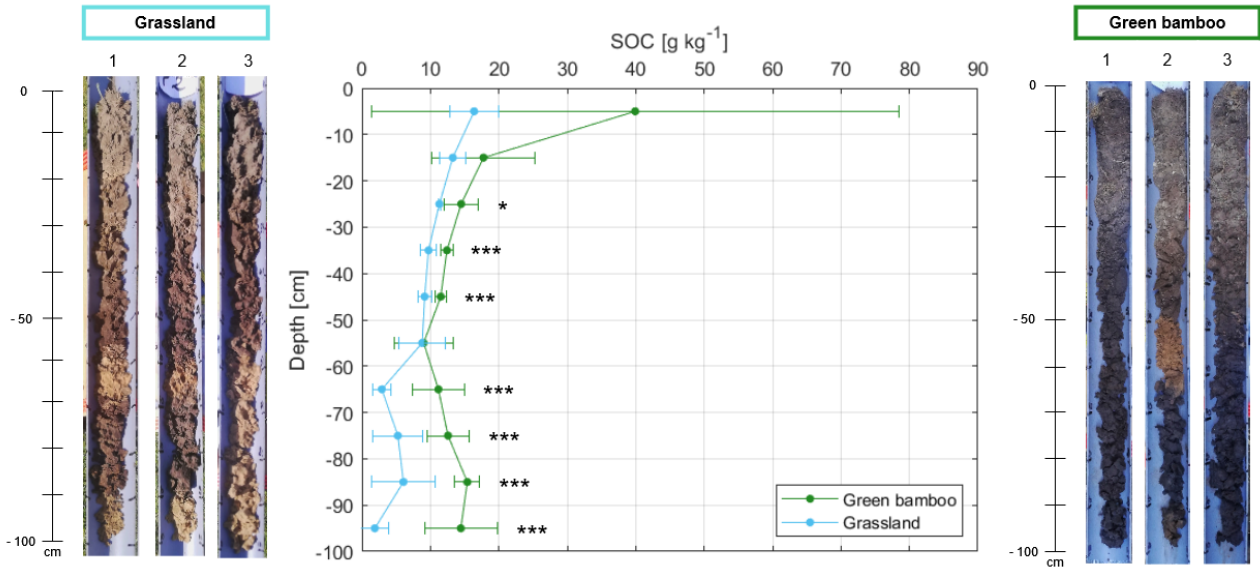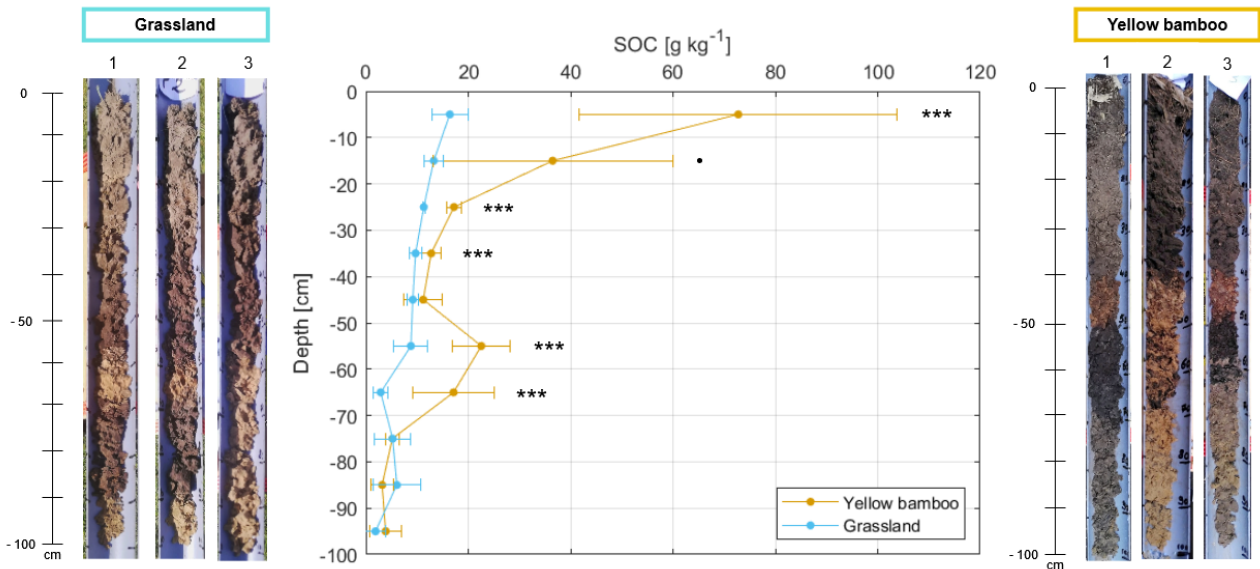

Figure 3.3: Comparison of the vertical distributions of SOC $[gC \ kg^{-1}]$ (mean $\pm$ standard deviation, n = 3) between the grassland and the yellow bamboo. The contents were obtained by dry combustion. Code (assuming a normal distribution): No symbol $p > 0.1$, $\bullet$ $p < 0.1$ (90% conf. level), $*$ $p < 0.05$ (95% conf. level), $**$ $p < 0.01$ (99% conf. level), $***$ $p < 0.001$

The system prospecting also revealed information of paramount importance: the presence of bamboo roots reaching down up to a depth of $40cm$. The grassland had only tiny, partially decomposed roots at that depth. In the system under consideration, the root-derived carbon thus mainly concerns the $0-40cm$ soil layer. It is essential information as root-derived carbon mainly supplies the stable soil carbon pools (Kätterer et al., 2011).

In order to better understand the dynamics of the system, Fe and Al analyses could be carried out within the B_h horizons and the C/metal ratio calculated. The organic matter dynamics is slow when the parent material is poor in nutrients, acidic or under waterlogging conditions. A greater accumulation of dissolved organic matter and dissolved root-derived organic carbon can be observed in the B_h horizon. Conversely, in soils where the parent material is rich in nutrients, dissolved organic carbon is more rapidly decomposed by microorganisms. The B_h horizon will contain less dissolved organic carbon and more iron and aluminium (Buurman and Jongmans, 2002; Buurman and Jongmans, 2005). Concerning the supposed paleosoil, carbon dating could be carried out to determine its age. However, all the analyses mentioned are outside the current work context.

Important note

The different soil profiles differ below a depth of $40cm$, especially in the position of the horizons. The origin of the organic matter below this limit remains a hypothesis. Furthermore, the roots of all three bamboo species stop at $40cm$, at which some root residues were also found in the grassland. Finally, it also seems that the concentrations measured at a depth of $0-40cm$ have a substantial standard deviation due to the low number of replicates per layer. For these reasons, the following analyses will only focus on the $0-40cm$ part of the system, and the lower layers are left out entirely.

3.2   Further investigation and biomass analysis

To start this thorough analysis, the SOC stock of the grassland is compared with the literature. The objective is to see how typical the grassland is of Zc (moderately drained sandy soil) in terms of SOC stock. Meersmans et al., 2008, calculated the evolution of SOC distribution with depth between 1960 and 2006 in northern Belgium. The interest here lies not in the change between these two dates but rather in the SOC stock in 2006, measured after a sampling campaign. Since their stock was quantified based on a $30cm$ depth, the SOC stock of the Merskplas grassland was recalculated based on the same thickness.

Table 3.1: Comparison between the Merksplas grassland and a typical $Zc-d$ one. The $0-30cm$ thickness is considered. Both values are presented with their corresponding standard error (SE)

Merksplas, 2022	Meersmans et al., 2008
SOC_{mass}	SOC_{mass}
$[kgC\ m^{-2}]$	$[kgC\ m^{-2}]$
6.09 ± 0.09	6.37 ± 0.78

Table 3.1 shows that the SOC stock of the Merksplas grassland is very similar to a reference grassland in Northern Belgium, as the two values overlap. However, this result must be interpreted with great caution as the two methodologies differ strongly. Firstly, Meersmans et al., 2008 used a pedo transfer function to calculate the bulk density. In addition, his organic carbon contents were obtained by the chemical titration method of Walkley & Black, and a correction factor of 1.33 was used. In the present work, we will not say that the Merksplas grassland is typical, but rather that the calculated stock is consistent with the literature. A detailed comparison with bamboo is therefore accurate.
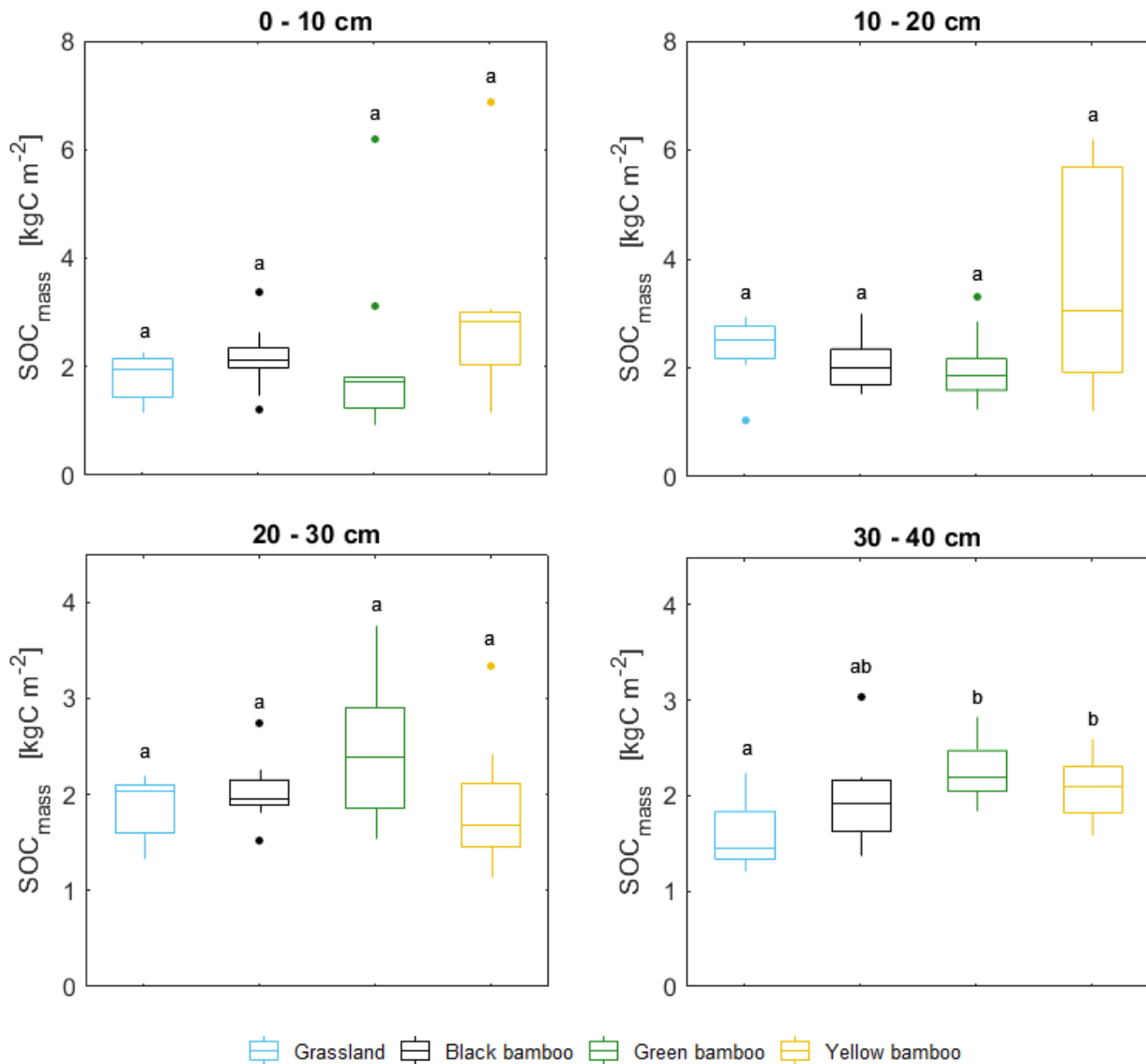

Figure 3.4: Boxplots and Dunn post-hoc test (Shapiro-Wilk, $p < 0.05$) showing the differences of SOC stock $[kgC\ m^{-2}]$ between grassland, black bamboo, green bamboo and yellow bamboo. Different letters indicate significant differences ($p < 0.05$). *The vertical axis scales are different.*

Table 3.2: Kruskal-Wallis test (Shapiro-Wilk, $p < 0.05$) results on SOC stocks

Depth	df	χ^2	p-value
$0-10cm$	3	8.30	0.112
$10-20cm$	3	9.36	0.095
$20-30cm$	3	9.73	0.090
$30-40cm$	3	30.9	0.003

After calculating the size effect (χ^2) (Tomczak and Tomczak, 2014), Table 3.2 shows that the type of plot (e.g. grassland or one bamboo species) has a weak effect ($\chi^2 < 14$)[1] on the SOC stock at $0-10cm$, $10-20cm$ and $20-30cm$. The respective p-values are all > 0.05, and the null hypothesis (H_0) can consequently not be rejected, which signifies that the means of the SOC stocks of grassland, black, green and yellow bamboo are similar. This is also confirmed by Figure 3.4, which, using the multiple pairwise comparison test, shows no significant difference between the SOC stocks for $0-10cm$, $10-20cm$ and $20-30cm$.

However, the results on the $30-40cm$ depth contrast with the previous ones. The last row of Table 3.2 indicates that vegetation type has a relatively strong effect on SOC stock for a depth of $30-40cm$. The p-value (< 0.05) allows to reject the null hypothesis H_0; therefore, the means are different. The multiple pairwise comparison test (Figure 3.4) indicates a significant difference ($p < 0.05$) between grassland and green bamboo, and between grassland and yellow bamboo, thus resulting in a SOC storage by the two bamboo species.

Though Figures 3.1, 3.2 and 3.3 showed some significant differences in SOC content [gC kg^{-1}], these differences cancel out over the first $30cm$ when calculating the SOC stock [kgC m^{-2}]. This is due to the consideration of the soil's bulk density ρ_s in each $10cm$ thickness. Table 3.3 shows firstly that bulk density increases with depth for each plot. This first trend is not surprising. Tsui et al., 2013, found that bulk density decreases significantly and linearly with SOC content [gC kg^{-1}], and increases with depth. Considering the $0-40cm$ depth, our first system prospecting validates this information.

Table 3.3: Measured bulk densities (mean $\pm$ standard deviation, n = 3). Within each depth, different letters indicate significant differences ($p < 0.05$) assuming a normal distribution

Depth [cm]	Grassland ρ_s [$kg\ m^{-3}$]	Black bamboo ρ_s [$kg\ m^{-3}$]	Green bamboo ρ_s [$kg\ m^{-3}$]	Yellow bamboo ρ_s [$kg\ m^{-3}$]
$0-10$	1131.34 ± 180.49 **a**	777.87 ± 124.93 **b**	737.07 ± 42.30 **b**	323.06 ± 57.29 **c**
$10-20$	1997.89 ± 112.55 **a**	1389.44 ± 152.47 **b**	1249.39 ± 130.68 **b**	994.67 ± 113.87 **c**
$20-30$	1898.94 ± 11.77 **a**	1610.70 ± 112.49 **b**	1759.31 ± 275.20 **ab**	1005.93 ± 356.34 **c**
$30-40$	1835.30 ± 72.86 **a**	1906.79 ± 46.67 **ab**	1961.33 ± 68.14 **bc**	1656.27 ± 46.48 **d**

---

[1]There is no formal way to determine a threshold value for the size effect. This value is mainly given as an indication from a rule of thumb.

For a Belgian sandy grassland, Mestdagh et al., 2006, measured a value of 1.26 ± 0.33 g cm^{-3} between 0 and $10cm$ depth and 1.42 ± 0.11 g cm^{-3} between 10 and $30cm$ depth by taking 8 samples for each of the two depths. Therefore, the bulk density values measured on the Merksplas grassland from $20cm$ depth would appear relatively high. Several hypotheses could explain this observation. Firstly, there is evidence that bulk density increases with compaction (Håkansson and Lipiec, 2000). However, there is no history of conventional agriculture on the site. Perhaps site activity, guided tours or other events could have raised this value, but this remains a hypothesis. Another possibility could be related to the low number of measurements (n = 3), although the standard deviations for the grassland are relatively restrained.

Furthermore, Table 3.3 also shows that over a depth of $0-20cm$, the bulk density of all bamboo species is significantly lower than that of grassland. The yellow bamboo has a significantly lower bulk density than the other vegetation types. In particular, its bulk density in the first $10cm$ is minimal. It is consistent with the site prospecting, which also revealed that this horizon was black and filled with tiny balls of very light organic material, rich in organic carbon, as shown in Figure 3.3. Don et al., 2011, found that after a minimum period of 7 years, a grassland transformed into a secondary forest lost on average $6.4 \pm 3.8\%$ of its bulk density in the first $30cm$. However, the effect of bamboo planting was not tested by the author.

In contrast to the SOC contents $[gC$ $kg^{-1}]$, bulk density values have strongly influenced the calculated SOC stocks $[kgC$ $m^{-2}]$. The standard deviations of the measured bulk densities are sometimes considerable, as shown by the yellow bamboo at $20-30cm$ depth. It, therefore, seems advisable to increase the number of replicates for bulk densities. For example, a series of ten soil replicates could be taken with the root auger. The SOC content and bulk density would then be measured for each sample. This approach, however, has little place in the botanical garden, given the limited size of the plots and their use for guided tours. Finally, it should be noted that the soil studied is very sandy and that, during sampling with the root auger, it was not uncommon for part of the sample to disintegrate and fall out of the sampled volume.

Biomass analysis

Table 3.4: Biomass measurements for the three bamboo species. *DBH*: different letters indicate significant differences ($p < 0.05$) according to Student's t-test (n = 40). *Leaves*: different letters indicate significant differences ($p < 0.05$) assuming a normal distribution (n = 3). Except for soil occupancy, the results represent the mean $\pm$ standard deviation

Plot	DBH	Soil occupancy	Leaves
	$[mm]$	$[\%]$	$[g]$
Black bamboo	15.72 ± 5.77 **a**	0.42	271.47 ± 134.22 **a**
Green bamboo	16.38 ± 5.41 **a**	0.35	143.47 ± 10.47 **a**
Yellow bamboo	36.92 ± 10.58 **b**	1.07	137.93 ± 11.90 **a**

Table 3.4 shows that yellow bamboo has a significantly higher diameter measured at breast height (DBH) than the other two species. It is related to the yellow bamboo's soil occupancy percentage, which indicates that the yellow bamboo culms cover 1.07% of the ground surface. Yellow bamboo has a lower planting density, but its culms are much wider and occupy a more significant percentage of the soil surface.

Moreover, Table 3.4 also shows no significant differences between the masses of the leaves gathered from the ground.
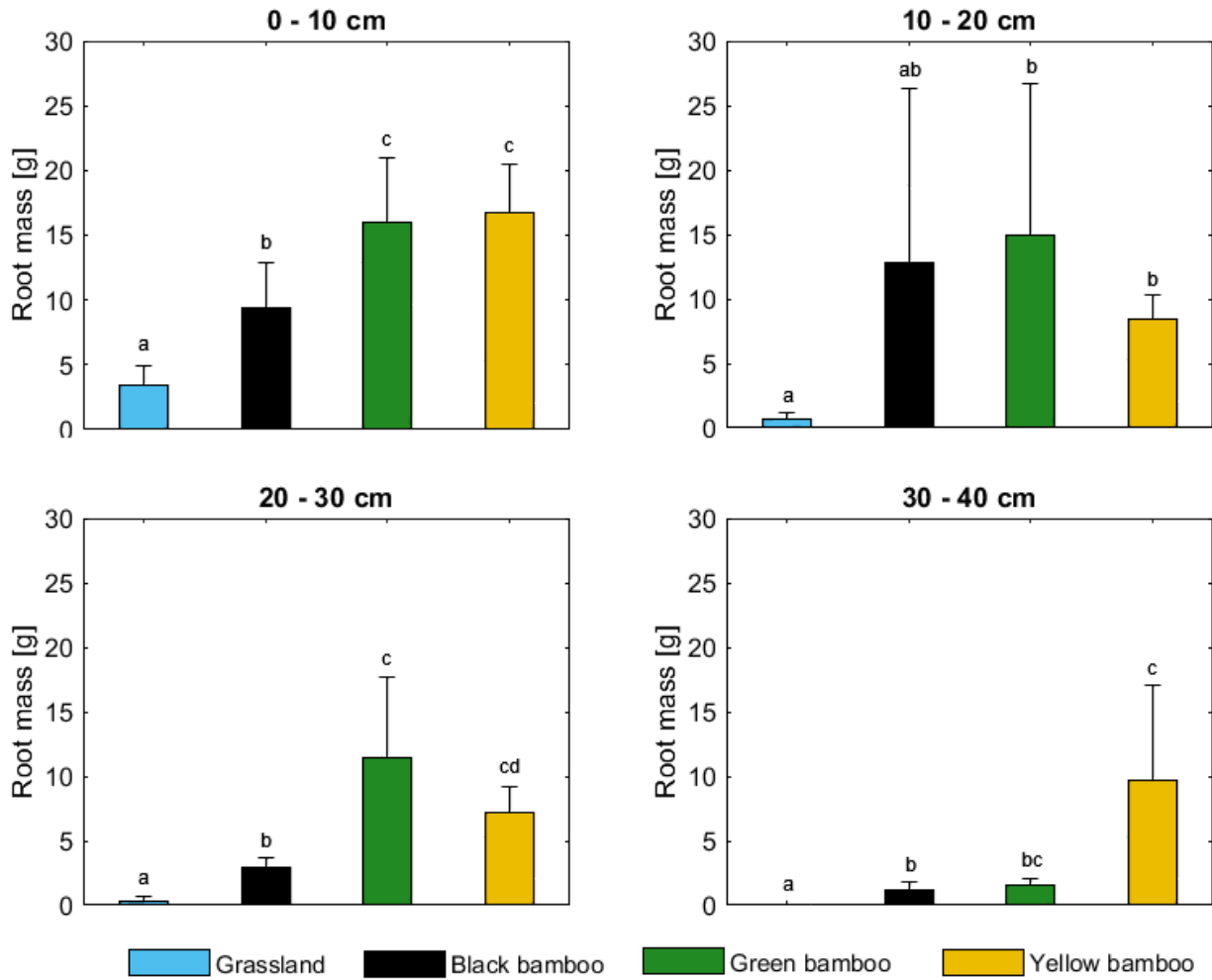
Figure 3.5: Root dry masses [g] (mean + standard deviation, n = 3) measured at four depths between grassland, black bamboo, green bamboo and yellow bamboo. Different letters indicate significant differences ($p < 0.05$) (95% conf. level) assuming a normal distribution. *The bar and standard deviation of the grassland at $30-40cm$ depth are too small to appear on the graph*

Finally, Figure 3.5 shows the root masses [g] collected at different depths within a volume[2] of $502.65cm^3$. First, the graph shows that bamboo has a significantly greater root mass than grassland, regardless of depth effect. It indicates that for the $0-30cm$ depth layer, no general trend is observable between the three bamboo species. One bamboo species has more roots on one layer, and another species has more roots on another layer. The large standard deviations can sometimes be explained by the presence of a large, relatively heavy rhizome. However, what is remarkable is that yellow bamboo is the only species with a stout rhizome at a depth of $30-40cm$. It is probably due to its higher soil occupancy rate, allowing it to develop its root system very profoundly. It could also explain why yellow bamboo has a significantly higher SOC stock than grassland and green bamboo at 30-40cm depth. On the other hand, the biomass measurements carried out for green bamboo do not justify with precision its higher SOC stock at $30-40cm$ depth.

---

[2]The actual volume of the root auger is greater. A black line was drawn to take only a 10-centimetre high soil layer, and the volume was therefore recalculated.

Walkley & Black

Table 3.5: One-way (regardless of the depth effect) and two-way ANOVA test (Shapiro-Wilk, $p > 0.05$; Levene, $p > 0.05$) results on correction factor (CF).

One-way				Two-way	
df	F	$p-value$		F	$p-value$
3	1.53	0.219	Vegetation−Depth	1.08	0.403
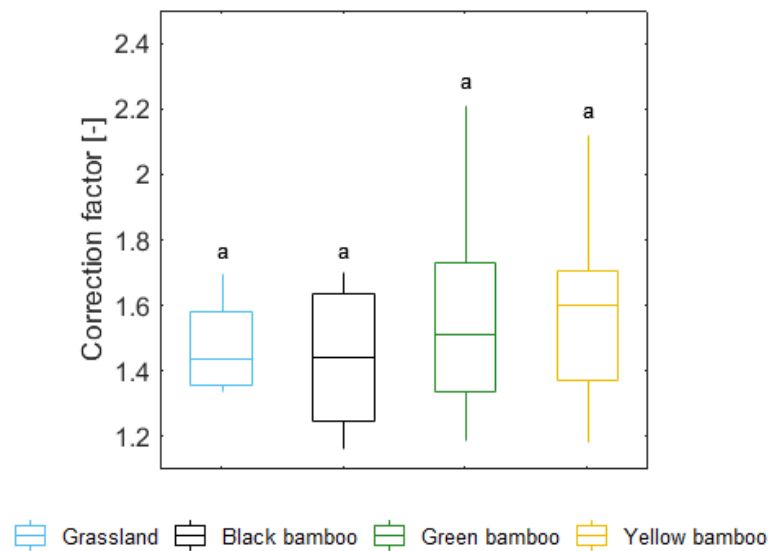
Figure 3.6: Boxplots and Tukey post-hoc test (Shapiro-Wilk, $p > 0.05$; Levene, $p > 0.05$) showing the differences of correction factors (CF) between grassland, black bamboo, green bamboo and yellow bamboo, regardless of the depth effect. Different letters indicate significant differences ($p < 0.05$)

The correction factor is the compensation for the incomplete oxidation of the Walkley & Black method (De Vos et al., 2007). When not separating the data by the depth and looking only at vegetation type, the one-way ANOVA (Table 3.5 - left) shows no significant differences in correction factors between the vegetation type ($p = 0.219$). The null hypothesis H_0 cannot be rejected and the CF means are similar. This result is confirmed by the post-hoc test shown in Figure 3.6. Moreover, the two-way ANOVA (Table 3.5 - right) shows no statistically significant interaction between vegetation type and depth for the correction factor ($p = 0.403$).

A significantly higher correction factor would have indicated a higher proportion of humic acids, charcoal or lignin-derived organic carbon (Lettens et al., 2007; Meersmans et al., 2009). This effect was not detected when analysing depths from 0 to $40cm$. Figure 3.6 also shows a broader spread of green and yellow bamboo correction factors. The reason could be that both vegetations had high SOC contents [gC kg^{-1}]. In this case, the Walkley & Black method is very sensitive and requires using a smaller soil mass (FAO, 2019). The correction factor calculated this way varies very quickly with the volume titrated. In addition, the colour change of the titration is sometimes difficult to detect accurately, which adds a user-related error.

A correction factor of 1.32 was introduced in the original Walkley & Black method (De Vos et al., 2007; Lettens et al., 2007). Since then, this value has been questioned, and the influence of soil use, texture and drainage has been demonstrated. For example, Meersmans et al., 2009 obtained a correction factor between 1.35 and 1.50 for a $Zc - d$ grassland in northern Belgium. The Figure 3.6 shows that the interquartile range of the grassland, i.e. 50% of its measured data, is in the same range as in the article. It again justifies that the Merskplas grassland is consistent with the literature and that the comparisons made are accurate.

3.3   Soil respiration analysis

As soil respiration depends on many environmental parameters (Faimon and Lang, 2018), the metadata for the measurements of each day are summarised in Appendix B. The metadata represent all the information related to the experiment and the environment in which it took place. It also ensures that the results are appropriately analysed for possible experiment replication. In this work, the metadata contain the parameters that could influence the CO_2 effluxes, i.e. start and end time of measurement, air temperature, relative humidity and precipitation.

Table 3.6: ANOVA (Shapiro-Wilk, $p > 0.05$; Levene, $p > 0.05$) and Welch's ANOVA (Shapiro-Wilk, $p > 0.05$; Levene, $p < 0.05$) test results on raw CO_2 efflux [$\mu mol \ m^{-2} \ s^{-1}$]

Date	Test	df	F	p-value
April 6	Welch's Anova	3	74.57	$7.252 \ 10^{-10}$
April 22	Welch's ANOVA	3	85.11	$1.65 \ 10^{-10}$
May 3	Welch's ANOVA	3	51.73	$1.559 \ 10^{-8}$
May 21	Welch's ANOVA	3	191.68	$1.026 \ 10^{-11}$
June 5	ANOVA	3	5.75	$2.920 \ 10^{-3}$
June 22	Welch's ANOVA	3	484.21	$6.505 \ 10^{-5}$

Table 3.7: ANOVA (Shapiro-Wilk, $p > 0.05$; Levene, $p > 0.05$), Welch's ANOVA (Shapiro-Wilk, $p > 0.05$; Levene, $p < 0.05$) and Kruskal-Wallis (Shapiro-Wilk, $p < 0.05$) test results on relative CO_2 efflux [$mgC \ g^{-1} \ hr^{-1}$]

Date	Test	df	F	χ^2	p-value
April 6	Welch's Anova	3	68.01	/	$9.423 \ 10^{-10}$
April 22	Kruskal-Wallis	3	/	79.20	$3.090 \ 10^{-6}$
May 3	Welch's ANOVA	3	42.32	/	$5.630 \ 10^{-8}$
May 21	ANOVA	3	165.70	/	$2.00 \ 10^{-11}$
June 5	ANOVA	3	43.93	/	$7.870 \ 10^{-4}$
June 22	ANOVA	3	502.60	/	$2.00 \ 10^{-16}$

Figure 3.7: Boxplots, Games-Howell (Shapiro-Wilk, $p > 0.05$; Levene, $p < 0.05$) and Tukey post-hoc tests (Shapiro-Wilk, $p > 0.05$; Levene, $p > 0.05$) showing the differences of CO_2 efflux [$\mu mol \; m^{-2} \; s^{-1}$] between grassland, black bamboo, green bamboo and yellow bamboo. Different letters indicate significant differences ($p < 0.05$). *The vertical axis scales are different.*

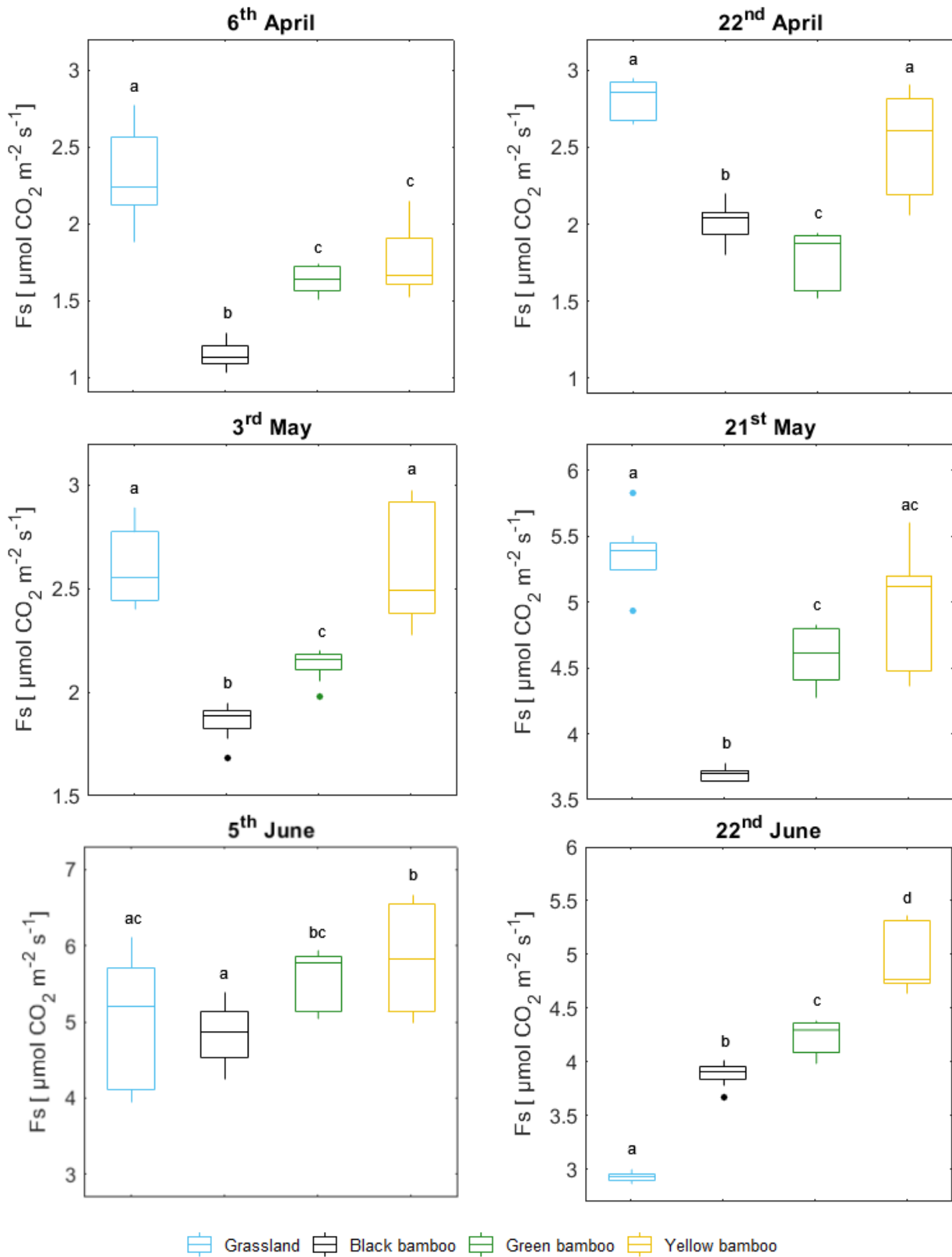Figure 3.8: Boxplots, Dunn (Shapiro-Wilk, $p < 0.05$), Games-Howell (Shapiro-Wilk, $p > 0.05$; Levene, $p < 0.05$) and Tukey post-hoc tests (Shapiro-Wilk, $p > 0.05$; Levene, $p > 0.05$) showing the differences of relative CO_2 efflux [$mgC\ g^{-1}\ hr^{-1}$] between grassland, black bamboo, green bamboo and yellow bamboo. Different letters indicate significant differences ($p < 0.05$). *The vertical axis scales are different.*
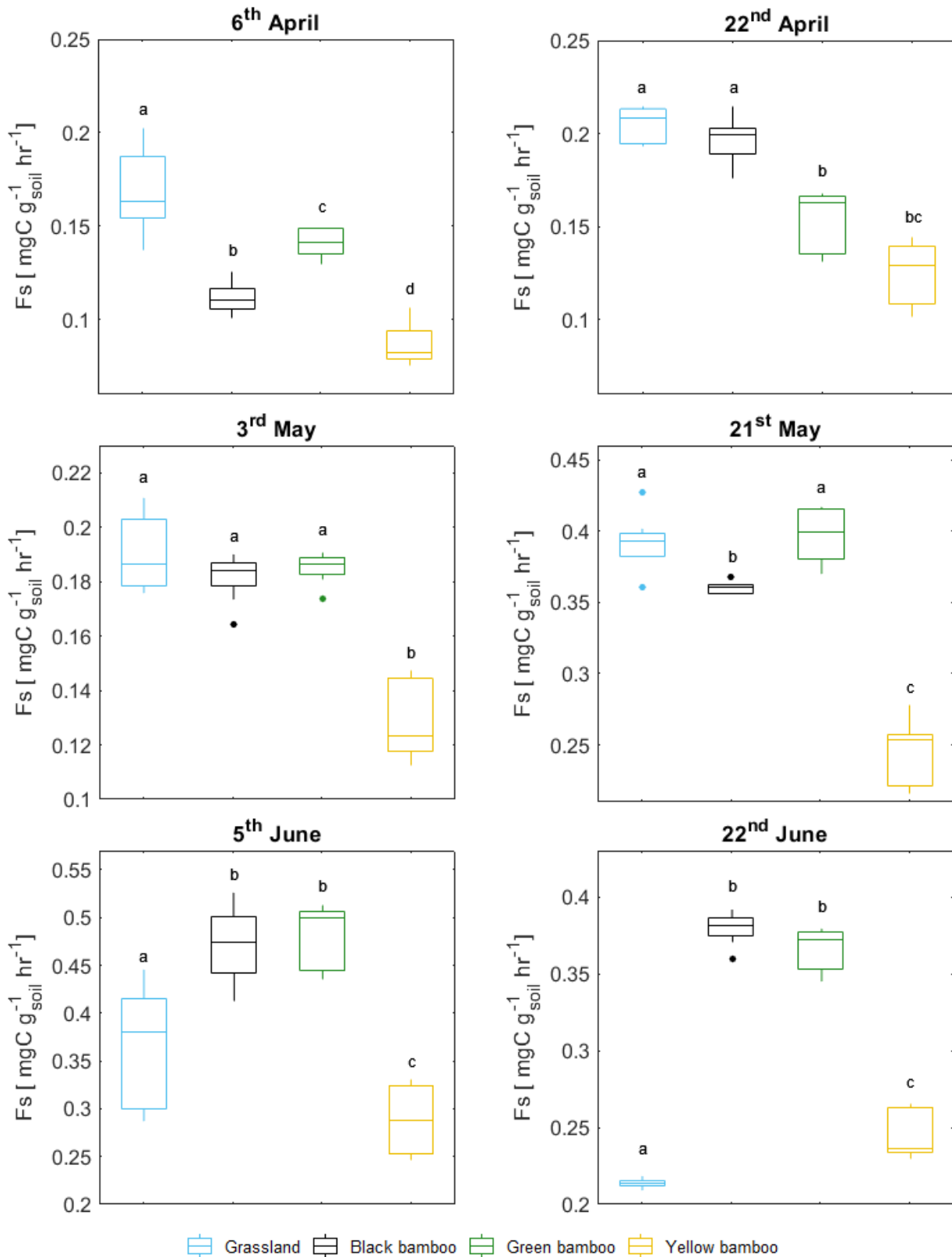
Statistical tests show that, for each date, the vegetation type significantly ($p < 0.05$) influences the raw CO_2 efflux [$\mu mol\ m^{-2}\ s^{-1}$] (Table 3.6) and the relative efflux [$mgC\ g^{-1}\ hr^{-1}$] (Table 3.7). The null hypothesis H_0 is therefore rejected, and the average CO_2 effluxes between vegetation types differ.

Firstly, Figure 3.7 shows that the order of magnitude of the raw CO_2 efflux measured on the grassland is the same as that obtained by Jérôme et al., 2014, who also studied a Belgian grassland (Dorinne). Though the author has used another measurement method (eddy covariance), it confirms that the unit transformation used is correct and supports the possibility of comparing the measured CO_2 effluxes between the different vegetation types.

The multiple comparison tests presented in Figure 3.7 do not show a clear trend. The one-to-one comparison of the vegetation types shows a lot of variability with significant differences. It is probably due to the low measurements representativeness on a longer time scale. Indeed, the CO_2 effluxes monitored in this work only cover a small time scale. This type of study is usually carried out using chamber systems or eddy covariance over several months (Bahn et al., 2008; Jérôme et al., 2012). The measurements are continuous over time, allowing a balance to be calculated over the measurement period covered.

Before analysing the relative CO_2 efflux [$mgC\ g^{-1}\ hr^{-1}$], it is essential to remember that these values were quantified by recalculating a stock based on the approximate insertion depth of the white collar. The new bulk density is not based on a depth of $10cm$. It is based on a new average bulk density value, measured with a Kopecky's ring at $4cm$ depth. This corresponds quite well to the insertion depth of the white collar in the soil. It is then considered that the measured soil respiration only comes from the soil inside the white collar.

The CO_2 efflux expressed in [$mgC\ g^{-1}\ hr^{-1}$] is a relative measure whose purpose is to consider the stability of organic carbon (Nuzzo et al., 2017). It, therefore, removes the effects of different SOC levels and represents the share of organic carbon respired by mineralisation. (Tian et al., 2016). This standardisation is not often used in the literature, where only a few studies take this factor into consideration. Indeed, it requires, in addition to monitoring the CO_2 efflux, sufficient measurements of soil SOC content. Nevertheless, some scientists have calculated relative CO_2 effluxes and obtained the same order of magnitude (Fissore et al., 2008; Nuzzo et al., 2017). This conclusion must be made with care because the soils studied differed from the Merksplas ones. However, it is reassuring that the equations used to standardise the CO_2 effluxes give similar results to the literature.

Figure 3.8 shows the multiple pairwise comparison test results. Several interesting points stand out. Firstly, five out of six measurements indicate that the relative CO_2 efflux of yellow bamboo is significantly lower ($p < 0.05$) than grassland's. The same result is observed between yellow and green bamboo. Secondly, for all measures, the relative CO_2 efflux is always significantly lower than that of black bamboo. Finally, no clear trend emerged from the green and black bamboo comparison. In other words, according to the six measurements, the SOC of yellow bamboo seems to be more stable than that of the grassland and the other two bamboo species.

By changing the relative abundance of labile and recalcitrant chemicals returned to the soil, litter amount and quality can impact SOC stability (Fissore et al., 2008). Due to either improved chemical stabilisation or physical protection in more difficult-to-access micro-aggregates, lignin or phenolic components inhibit soil CO_2 efflux and make it harder for soil microorganisms to mineralize SOC (Nuzzo et al., 2017).

The Walkley & Black chemical titration could have detected a variation in the complexity of the mineralised organic molecules. Though the yellow bamboo boxplot covers a higher range of correction factors (CF), no significant difference was found. It can, however, be attributed to the small number of samples from each group used in the chemical analysis.

Finally, these variations in relative CO_2 effluxes are studied considering the two environmental parameters measured. Table 3.8 presents the results of the two ANCOVA tests. The ANCOVA tests whether the independant variable, i.e. the vegetation type, still influences the response variable, i.e. the CO_2 efflux, after removing the influence of the covariate. The first covariate is the soil temperature (T_{soil}), and the second one is the gravimetric water (GWC). The results below should be interpreted with care as the normality and equality of variance assumptions were not always met. However, there is no simple non-parametric alternative to ANCOVA. The results below are offered for discussion.

Table 3.8: ANCOVA test results on relative CO_2 efflux [$mgC\ g^{-1}\ hr^{-1}$]

	F	p-value		F	p-value
Vegetation type	14.04	$3.363\ 10^{-7}$	Vegetation type	3.19	0.029
T_{soil}	90.52	$4.630\ 10^{-14}$	GWC	1.18	0.280

The soil temperature covariate is significantly related to the CO_2 efflux (F = 90.52; $p < 0.05$). The vegetation type also significantly impacts the CO_2 efflux after controlling for the soil temperature effect (F = 14.04; $p < 0.05$).

The gravimetric water content covariate does not significantly impact the CO_2 efflux (F = 1.18; $p > 0.05$). However, after controlling for its effect, the vegetation type still significantly impacts the CO_2 efflux (F = 3.19; $p < 0.05$).

In other words, by removing the effect of temperature, i.e. the first covariate, the vegetation type still has a significant impact on CO_2 efflux. The same conclusion is drawn by eliminating the effect of gravimetric water content. The multiple pairwise comparison post-hoc test gives the following results.

Table 3.9: ANCOVA post-hoc test results on relative CO_2 efflux [$mgC\ g^{-1}\ hr^{-1}$]

	Covariate	T_{soil}	GWC
Comparison		p-value	p-value
Grassland − Black bamboo		< 0.001	0.9161
Grassland − Green bamboo		< 0.001	0.766
Grassland − Yellow bamboo		0.765	0.265
Green bamboo − Black bamboo		0.978	0.986
Green bamboo − Yellow bamboo		< 0.001	0.0317
Yellow bamboo − Black bamboo		< 0.001	0.071

Table 3.9 should be interpreted as follows. Black bamboo and green bamboo lead to a statistically significantly different ($p < 0.001$) CO_2 efflux compared to grassland, even after controlling for the soil temperature. However, this conclusion does not work for gravimetric water content ($p = 0.9161$ and 0.766). When p is > 0.05, this means that by removing the effect of the covariate, the vegetation type no longer significantly impacts the CO_2 efflux.

Finally, it is appropriate to say that the vegetation type influences the CO_2 efflux measurements, even after controlling for temperature and gravimetric water content. Regardless of the effect of the covariate, a significant difference in CO_2 efflux is thus observed between the vegetation types. It is a general conclusion on the whole dataset. An explanation for the CO_2 efflux variations between two vegetation types could be the quality of the SOC. The SOC derives from the bamboo's many highly developed roots and leaves, which is not the case for the grassland. This effect, however, is not quantified by the ANCOVA. The post-hoc test shows that these two covariables might sometimes directly be responsible for CO_2 efflux variations ($p > 0.05$). This trend is logical in practice, as bamboo has a well-developed canopy, creating shade and preventing the soil from heating up.
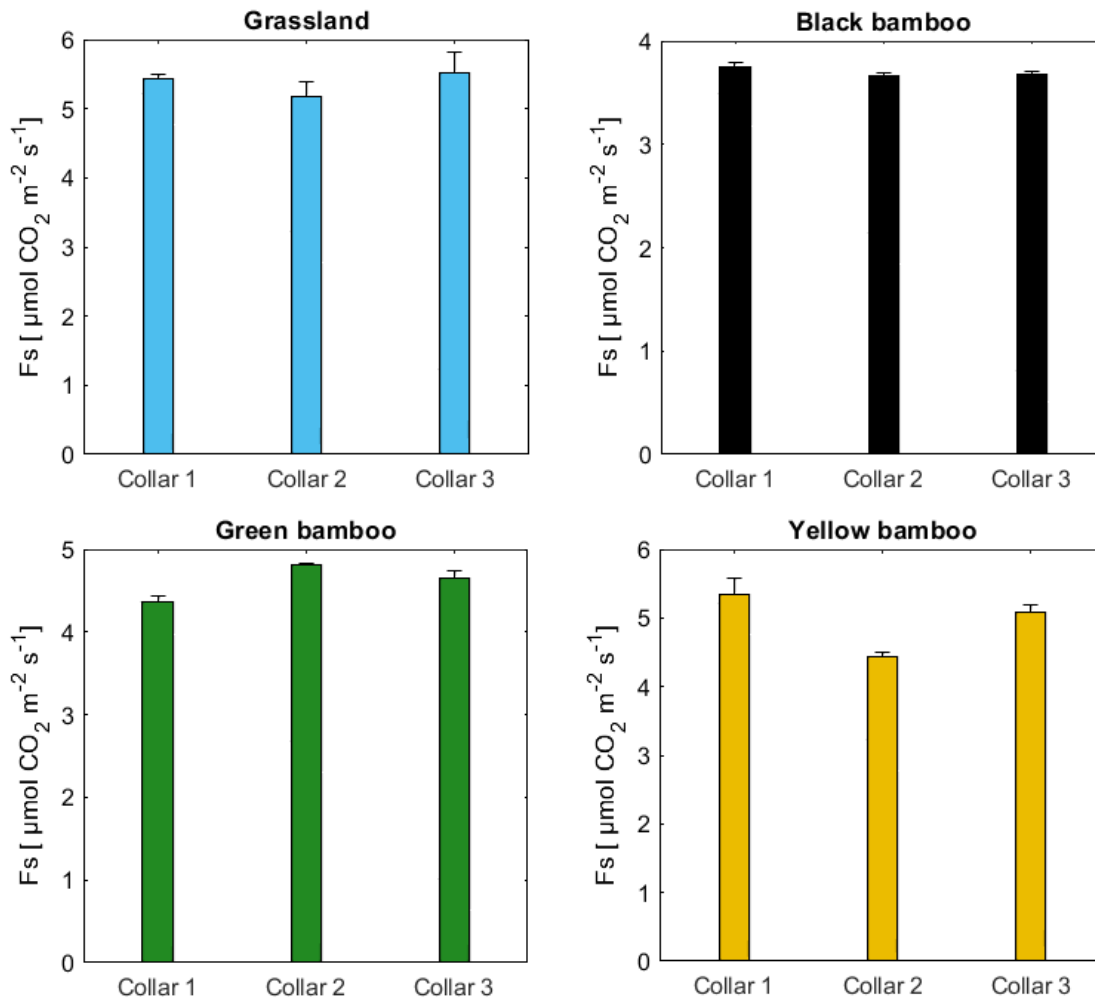
Efflux variability

Figure 3.9: CO_2 efflux variability (mean + standard deviation, n = 3 for each collar). The graphs only represent the 21st May

For a possible replication of the experiment, it is interesting to know the variability of the CO_2 efflux measurements. Figure 3.9 represents the variability measured on each white collar on 21 May 2022. Since the standard deviation is minimal for each white collar, the variability within each white collar is very low. The same trend was observed every measurement day when processing the data. Therefore, performing several repetitions on the same white collar is unnecessary.

3.3.1   SOC stock variation

One of the objectives of the work was to assess whether there was a significant difference in SOC stock $[kgC \ m^{-2}]$ when moving from a grassland to a bamboo plantation. After analysing the differences in the previous sections, it is interesting to keep in mind an order of magnitude. Table 3.10 shows the SOC stock variations only for the significant depths.

Table 3.10: SOC stock variation between a grassland and three bamboo plantations. The indicated value is the difference between two means (n = 10). n.s. = not significant

	Depth 0−10cm	Depth 10−20cm	Depth 20−30cm	Depth 30−40cm
Grassland ⟶ Black bamboo	n.s.	n.s.	n.s.	n.s.
Grassland ⟶ Green bamboo	n.s.	n.s.	n.s.	+ 0.69 $[kgC \ m^{-2}]$
Grassland ⟶ Yellow bamboo	n.s.	n.s.	n.s.	+ 0.51 $[kgC \ m^{-2}]$

To finish this analysis, it may be interesting to have a measured SOC stock value on each vegetation type. Though some depths did not show a significant difference, the stock calculated over 40 centimetres can be used as a comparison for other researchers. Table 3.11 shows the average stock calculated by adding the stock of each layer.

Table 3.11: SOC stock for each vegetation type. The value is based on a depth of 0−40cm

	$SOC_{mass} \ [kgC \ m^{-2}]$
Grassland	7.66
Black bamboo	8.28
Green bamboo	8.87
Yellow bamboo	10.33

For comparison, Chen et al., 2009, found[3] a stock of 9.02 $[kgC \ m^{-2}]$ for a Chinese bamboo forest. The comparison should be interpreted with care. First, the Chinese climate and forest context differ from the Belgian botanical garden. Secondly, the author's analyses were carried out by chemical methods. It is still interesting to note that the order of magnitude is similar. Finally, the author states that most of the SOC was stored in the first $40cm$, which supports the sampling method used in this work and brings this analysis to a close.

---

[3]This value was calculated based on the SOC contents $[gC \ kg^{-1}]$ and bulk densities measured by the author.

Chapter 4

Conclusion & Prospects

4.1 Conclusion

Many parameters were investigated in this master's thesis in order to compare different organic carbon dynamics after a grassland has been converted into a plantation of several bamboo species. An initial prospecting of the system limited the depth of interest to between 0 and $40cm$.

Though the average SOC contents were globally higher in each of the bamboo plantations than in the grassland, only two bamboo species showed a significantly higher SOC stock between 30 and $40cm$ depth. It is due to the consideration of soil bulk densities which were lower in bamboo than in grassland. For yellow bamboo, this increase in stock could be due to a larger average culm diameter, resulting in a higher soil occupancy rate and a significantly more developed root system at depth. The biomass analysis of green bamboo failed to support this increase in stock.

The whole dataset showed that after removing the effect of temperature or gravimetric water content, the vegetation type still significantly influenced the relative CO_2 efflux. It may be due to a difference in the chemical composition of SOC between grassland and bamboo. The correction factor analysis did not reveal this difference, probably due to the low number of replicates or laboratory error. Finally, overall, the CO_2 effluxes of yellow bamboo were significantly lower than those of grassland and the other two bamboo species, resulting in better SOC stability.

4.2 Prospects

In view of the work done, some recommendations come to mind. Firstly, increasing the number of bulk density measurements seems sensible, mainly as this strongly influences the SOC stock. If the same type of experiment were to be carried out in a forest, it would seem appropriate to take each soil sample with a root auger, provided that the logistics allow for this.

Secondly, increasing the number of CO_2 measurements in winter would be interesting. The measures made cover only one cold winter day and five warmer days. This idea would give a better temporal representation of the system studied. Chamber measurements could be considered in order to have continuous efflux measurements over time, both day and night.

Given the low variability of the CO_2 efflux within the same white collar, it is recommended to perform only one measurement per white collar and to increase the number of white collars. It would also increase the independence of the different measured values.

A better knowledge of the dynamics of the organic matter entering the system could be obtained by carrying out, for example, a thorough study on the degradation of the bamboo litter, or by installing nets to harvest the leaves. However, these experiments are time-consuming and require the organisation of another project dedicated to this topic.

Finally, the results obtained in this work open the door to other experiments that could, for example, be carried out in forests, where bamboo culms are generally more developed. An increase in SOC stock was detected in green and yellow bamboo. If more extended experiments are carried out, it could introduce a possible carbon reward based on storing organic carbon in the soil. The present study is, therefore, complementary to the various experiments aimed at quantifying the sequestration of atmospheric carbon in the aerial parts of the bamboo.

Contribution

Jeroen Meersmans and I took all soil samples. I then dried, sieved and crushed them. The agricultural soil testing laboratory of La Hulpe conducted the organic carbon analyses by dry combustion. I measured organic carbon content by chemical titration (Walkley & Black), performed statistical analyses, and measured bulk density and root masses. Finally, all soil respiration measurements were carried out by me, accompanied by Jeroen Meersmans or my father.

An information sheet per plot was also produced and displayed on site to inform the public. I created them, and Jeroen Meersmans proofread them. After this master thesis, a poster will be exhibited in the botanical garden.

References

Al-Ghussain, L. (2018). Global warming: Review on driving forces and mitigation. *Environmental Progress*, 9.

Bahn, M., Rodeghiero, M., Anderson-Dunn, M., Dore, S., Gimeno, C., Drösler, M., Williams, M., Ammann, C., Berninger, F., Flechard, C., Jones, S., Balzarolo, M., Kumar, S., Newesely, C., Priwitzer, T., Raschi, A., Siegwolf, R., Susiluoto, S., Tenhunen, J., . . . Cernusca, A. (2008). Soil Respiration in European Grasslands in Relation to Climate and Assimilate Supply. *Ecosystems*, *11*(8), 1352–1367. https://doi.org/10.1007/s10021-008-9198-0

Basak, M., Dutta, S., Biswas, S., Chakraborty, S., Sarkar, A., Rahaman, T., Dey, S., Biswas, P., & Das, M. (2021). Genomic insights into growth and development of bamboos: What have we learnt and what more to discover? *Trees*, *35*(6), 1771–1791. https://doi.org/10.1007/s00468-021-02197-6

Bispo, A., Andersen, L., Angers, D. A., Bernoux, M., Brossard, M., Cécillon, L., Comans, R. N. J., Harmsen, J., Jonassen, K., Lamé, F., Lhuillery, C., Maly, S., Martin, E., Mcelnea, A. E., Sakai, H., Watabe, Y., & Eglin, T. K. (2017). Accounting for Carbon Stocks in Soils and Measuring GHGs Emission Fluxes from Soils: Do We Have the Necessary Standards? *Frontiers in Environmental Science*, *5*, 41. https://doi.org/10.3389/fenvs.2017.00041

Bogemans, F. (Ed.). (2005). *Toelichting bij de Quartairgeologische Kaart 2-8 Meerle - Turnhout*. Vlaamse overheid Dienst Natuurlijke Rijkdommen.

Buurman, P., & Jongmans, A. G. (2002). Podzolization - An additional paradigm. *EDAFOLOGIA*, *9*(2), 107–114.

Buurman, P., & Jongmans, A. (2005). Podzolisation and soil organic matter dynamics. *Geoderma*, *125*(1-2), 71–83. https://doi.org/10.1016/j.geoderma.2004.07.006

Capparelli, G., Spolverino, G., & Greco, R. (2018). Experimental Determination of TDR Calibration Relationship for Pyroclastic Ashes of Campania (Italy). *Sensors*, *18*(11), 3727. https://doi.org/10.3390/s18113727

Chen, X., Zhang, X., Zhang, Y., Booth, T., & He, X. (2009). Changes of carbon stocks in bamboo stands in China during 100 years. *Forest Ecology and Management*, *258*(7), 1489–1496. https://doi.org/10.1016/j.foreco.2009.06.051

Chenu, C., Angers, D. A., Barré, P., Derrien, D., Arrouays, D., & Balesdent, J. (2019). Increasing organic stocks in agricultural soils: Knowledge gaps and potential innovations. *Soil and Tillage Research*, *188*, 41–52. https://doi.org/10.1016/j.still.2018.04.011

Chenu, C., Klumpp, K., Bispo, A., Angers, D., Colnenne, C., & Metay, A. (2014). Stocker du carbone dans les sols agricoles: Évaluation de leviers d'action pour la France, 16.

Cobos, D. R. (n.d.). Calibrating ECH2O Soil Moisture Sensors. *Decagon Devices*, 8.

Databank Ondergrond Vlaanderen. (2017). Retrieved June 3, 2022, from https://www.dov.vlaanderen.be/geonetwork/srv/fre/catalog.search#/metadata/a1547a01-b9fc-40fa-a2eb-009a39c02c7b

Databank Ondergrond Vlaanderen. (2020). Retrieved June 2, 2022, from https://www.dov.vlaanderen.be/portaal/?module=verkenner&bm=e15e8cd8-b677-45a1-9148-6fa4b111520b

De Vos, B., Lettens, S., Muys, B., & Deckers, J. A. (2007). Walkley and Black analysis of forest soil organic carbon: Recovery, limitations and uncertainty. *Soil Use and Management*, *23*(3), 221–229. https://doi.org/10.1111/j.1475-2743.2007.00084.x

Deluz, C., Nussbaum, M., Sauzet, O., Gondret, K., & Boivin, P. (2020). Evaluation of the Potential for Soil Organic Carbon Content Monitoring With Farmers. *Frontiers in Environmental Science*, *8*, 113. https://doi.org/10.3389/fenvs.2020.00113

Don, A., Schumacher, J., & Freibauer, A. (2011). Impact of tropical land-use change on soil organic carbon stocks - a meta-analysis: SOIL ORGANIC CARBON AND LAND-USE CHANGE. *Global Change Biology*, *17*(4), 1658–1670. https://doi.org/10.1111/j.1365-2486.2010.02336.x

Faimon, J., & Lang, M. (2018). What actually controls the minute to hour changes in soil carbon dioxide concentrations? *Geoderma*, *323*, 52–64. https://doi.org/10.1016/j.geoderma.2018.02.048

FAO. (2019). Standard operating procedure for soil organic carbon. Walkley-Black method: Titration and colorimetric method, 27.

Fissore, C., Giardina, C. P., Kolka, R. K., Trettin, C. C., King, G. M., Jurgensen, M. F., Barton, C. D., & Mcdowell, S. D. (2008). Temperature and vegetation effects on soil organic carbon quality along a forested mean annual temperature gradient in North America: TEMPERATURE AND VEGETATION EFFECTS ON SOC QUALITY. *Global Change Biology*, *14*(1), 193–205. https://doi.org/10.1111/j.1365-2486.2007.01478.x

Fu, W., Jiang, P., Zhao, K., Zhou, G., Li, Y., Wu, J., & Du, H. (2014). The carbon storage in moso bamboo plantation and its spatial variation in Anji County of southeastern China. *Journal of Soils and Sediments*, *14*(2), 320–329. https://doi.org/10.1007/s11368-013-0665-7

Gangwar, T., & Schillinger, D. (2019). Microimaging-informed continuum micromechanics accurately predicts macroscopic stiffness and strength properties of hierarchical plant culm

materials. *Mechanics of Materials*, *130*, 39–57. https://doi.org/10.1016/j.mechmat.2019.01.009

Geopunt Vlaanderen, G. V. (2022). Retrieved March 17, 2022, from https://www.geopunt.be/

Gevangenismuseum, G. (n.d.). Retrieved June 12, 2022, from http://www.gevangenismuseum.be/merksplas-kolonie.html

Håkansson, I., & Lipiec, J. (2000). A review of the usefulness of relative bulk density values in studies of soil structure and compaction. *Soil and Tillage Research*, *53*(2), 71–85. https://doi.org/10.1016/S0167-1987(99)00095-1

Henry, M., Bombelli, A., Trotta, C., Alessandrini, A., Birigazzi, L., Sola, G., Vieilledent, G., Santenoise, P., Longuetaud, F., Valentini, R., Picard, N., & Saint-André, L. (2013). GlobAllomeTree: International platform for tree allometric equations to support volume, biomass and carbon assessment. *iForest - Biogeosciences and Forestry*, *6*(6), 326–330. https://doi.org/10.3832/ifor0901-006

Humanitarian, B. (2009). *A manual on the humanitarian use of bamboo in Indonesia*. Chapman & Hall/CRC Press.

IRM, I. (n.d.). Retrieved June 8, 2022, from https://www.meteo.be/fr/climat/climat-de-la-belgique/climat-dans-votre-commune

Jérôme, E., Beckers, Y., Bodson, B., Dumortier, P., van, J. B., Heinesch, B., Moureaux, C., & Aubinet, M. (2012). Agriculture et changements climatiques : Bilan de carbone d'une prairie pâturée en Région wallonne., 7.

Jérôme, E., Beckers, Y., Bodson, B., Heinesch, B., Moureaux, C., & Aubinet, M. (2014). Impact of grazing on carbon dioxide exchanges in an intensively managed Belgian grassland. *Agriculture, Ecosystems & Environment*, *194*, 7–16. https://doi.org/10.1016/j.agee.2014.04.021

Kätterer, T., Bolinder, M. A., Andrén, O., Kirchmann, H., & Menichetti, L. (2011). Roots contribute more to refractory soil organic matter than above-ground crop residues, as revealed by a long-term field experiment. *Agriculture, Ecosystems & Environment*, *141*(1-2), 184–192. https://doi.org/10.1016/j.agee.2011.02.029

Kim, M.-I., Chae, B.-G., & Nishigaki, M. (2008). Evaluation of geotechnical properties of saturated soil using dielectric responses. *Geosciences Journal*, *12*(1), 83–93. https://doi.org/10.1007/s12303-008-0010-0

Krettek, A., & Rennert, T. (2021). Mobilisation of Al, Fe, and DOM from topsoil during simulated early Podzol development and subsequent DOM adsorption on model minerals. *Scientific Reports*, *11*(1), 19741. https://doi.org/10.1038/s41598-021-99365-y

Lal, R. (2004). Soil carbon sequestration to mitigate climate change. *Geoderma*, *123*(1-2), 1–22. https://doi.org/10.1016/j.geoderma.2004.01.032

Lal, R. (2013). Soil carbon management and climate change. *Carbon Management*, *4*(4), 439–462. https://doi.org/10.4155/cmt.13.31

Le Quéré, C., Moriarty, R., Andrew, R. M., Canadell, J. G., Sitch, S., Korsbakken, J. I., Friedlingstein, P., Peters, G. P., Andres, R. J., Boden, T. A., Houghton, R. A., House, J. I., Keeling, R. F., Tans, P., & Arneth, A. (2015). Global Carbon Budget 2015. *Earth System Science Data*, *7*(2), 349–396. https://doi.org/10.5194/essd-7-349-2015

Lehmann, J., & Kleber, M. (2015). The contentious nature of soil organic matter. *Nature*, *528*(7580), 60–68. https://doi.org/10.1038/nature16069

Lettens, S., De Vos, B., Quataert, P., van Wesemael, B., Muys, B., & van Orshoven, J. (2007). Variable carbon recovery of Walkley-Black analysis and implications for national soil organic carbon accounting. *European Journal of Soil Science*, *58*(6), 1244–1253. https://doi.org/10.1111/j.1365-2389.2007.00916.x

Li, P., Zhou, G., Du, H., Lu, D., Mo, L., Xu, X., Shi, Y., & Zhou, Y. (2015). Current and potential carbon stocks in Moso bamboo forests in China. *Journal of Environmental Management*, *156*, 89–96. https://doi.org/10.1016/j.jenvman.2015.03.030

Liese, W., & Köhl, M. (Eds.). (2015). *Bamboo: The Plant and its Uses* (Vol. 10). Springer International Publishing. https://doi.org/10.1007/978-3-319-14133-6

Lin, Z., Li, Y., Tang, C., Luo, Y., Fu, W., Cai, X., Li, Y., Yue, T., Jiang, P., Hu, S., & Chang, S. X. (2018). Converting natural evergreen broadleaf forests to intensively managed moso bamboo plantations affects the pool size and stability of soil organic carbon and enzyme activities. *Biology and Fertility of Soils*, *54*(4), 467–480. https://doi.org/10.1007/s00374-018-1275-8

Longdoz, B., Yernaux, M., & Aubinet, M. (2000). Soil CO_2 efflux measurements in a mixed forest: Impact of chamber disturbances, spatial variability and seasonal evolution. *Global Change Biology*, *6*(8), 907–917. https://doi.org/10.1046/j.1365-2486.2000.00369.x

Longdoz, B. (2021). *Exchanges Ecosystems-Atmosphere under Climate Change. Academic course taught at the University of Gembloux Agro-Bio tech.*

Maier, M., Schack-Kirchner, H., Hildebrand, E., & Schindler, D. (2011). Soil CO2 efflux vs. soil respiration: Implications for flux models. *Agricultural and Forest Meteorology*, *151*(12), 1723–1730. https://doi.org/10.1016/j.agrformet.2011.07.006

McAdam, S. A., & Brodribb, T. J. (2015). The Evolution of Mechanisms Driving the Stomatal Response to Vapor Pressure Deficit. *Plant Physiology*, *167*(3), 833–843. https://doi.org/10.1104/pp.114.252940

Meersmans, J., De Ridder, F., Canters, F., De Baets, S., & Van Molle, M. (2007). A multiple regression approach to assess the spatial distribution of Soil Organic Carbon (SOC) at the regional scale (Flanders, Belgium). *Geoderma*, *143*(1-2), 1–13. https://doi.org/10.1016/j.geoderma.2007.08.025

Meersmans, J., Van Wesemael, B., De Ridder, F., Fallas Dotti, M., De Baets, S., & Van Molle, M. (2008). Changes in organic carbon distribution with depth in agricultural soils in northern Belgium, 1960–2006. *Global Change Biology, 15*(11), 2739–2750. https://doi.org/10.1111/j.1365-2486.2009.01855.x

Meersmans, J., Van Wesemael, B., Goidts, E., Van Molle, M., De Baets, S., & De Ridder, F. (2011). Spatial analysis of soil organic carbon evolution in Belgian croplands and grasslands, 1960-2006. *Global Change Biology, 17*(1), 466–479. https://doi.org/10.1111/j.1365-2486.2010.02183.x

Meersmans, J., Van Wesemael, B., & Van Molle, M. (2009). Determining soil organic carbon for agricultural soils: A comparison between the Walkley & Black and the dry combustion methods (north Belgium). *Soil Use and Management, 25*(4), 346–353. https://doi.org/10.1111/j.1475-2743.2009.00242.x

Melillo, J. M., Steudler, P. A., Aber, J. D., Newkirk, K., Lux, H., Bowles, F. P., Catricala, C., Magill, A., Ahrens, T., & Morrisseau, S. (2002). Soil Warming and Carbon-Cycle Feedbacks to the Climate System. *Science, 298*(5601), 2173–2176. https://doi.org/10.1126/science.1074153

Mestdagh, I., Lootens, P., Van Cleemput, O., & Carlier, L. (2006). Variation in organic-carbon concentration and bulk density in Flemish grassland soils. *Journal of Plant Nutrition and Soil Science, 169*(5), 616–622. https://doi.org/10.1002/jpln.200521861

Meter Group. (n.d.). Retrieved April 9, 2022, from https://www.metergroup.com/en/meter-environment/measurement-insights/tdr-fdr-capacitance-compared

Minasny, B., McBratney, A. B., Mendonça-Santos, M. L., Odeh, I. O. A., & Guyon, B. (2006). Prediction and digital mapping of soil carbon storage in the Lower Namoi Valley. *Soil Research, 44*(3), 233. https://doi.org/10.1071/SR05136

Mirmehdi, M. (2016). The Effects of bamboo species and adhesive type on mechanical properties of laminated bamboo lumber (LBL) [Publisher: Unpublished]. https://doi.org/10.13140/RG.2.1.2363.6881

Mokma, D., Yli-Halla, M., & Lindqvist, K. (2004). Podzol formation in sandy soils of Finland. *Geoderma, 120*(3-4), 259–272. https://doi.org/10.1016/j.geoderma.2003.09.008

Morais, T. G., Teixeira, R. F., & Domingos, T. (2019). Detailed global modelling of soil organic carbon in cropland, grassland and forest soils (D. Sihi, Ed.). *PLOS ONE, 14*(9), e0222604. https://doi.org/10.1371/journal.pone.0222604

Ngao, J., Longdoz, B., Granier, A., & Epron, D. (2007). Estimation of autotrophic and heterotrophic components of soil respiration by trenching is sensitive to corrections for root decomposition and changes in soil water content. *Plant and Soil, 301*(1-2), 99–110. https://doi.org/10.1007/s11104-007-9425-z

Nuzzo, A., Spaccini, R., Cozzolino, V., Moschetti, G., & Piccolo, A. (2017). In situ polymerization of soil organic matter by oxidative biomimetic catalysis. *Chemical and Biological Technologies in Agriculture, 4*(1), 12. https://doi.org/10.1186/s40538-017-0094-8

Ontl, T., & Schulte, T. (2012). Soil carbon storage. *Nature Education Knowledge*, *3*(10), 35.

Panepinto, D., Riggio, V. A., & Zanetti, M. (2021). Analysis of the Emergent Climate Change Mitigation Technologies. *International Journal of Environmental Research and Public Health*, *18*(13), 6767. https://doi.org/10.3390/ijerph18136767

Paustian, K., Lehmann, J., Ogle, S., Reay, D., Robertson, G. P., & Smith, P. (2016). Climate-smart soils. *Nature*, *532*(7597), 49–57. https://doi.org/10.1038/nature17174

Plantentuin Merksplas. (2022). Retrieved June 6, 2022, from http://plantentuinmerksplas.be/onze-tuin/geschiedenis/

Prayogo, C., Muthahar, C., & Ishaq, R. M. (2021). Allometric equation of local bamboo for estimating carbon sequestration of bamboo riparian forest. *IOP Conference Series: Earth and Environmental Science*, *905*(1), 012002. https://doi.org/10.1088/1755-1315/905/1/012002

Ritchie, R. J. (2010). Modelling photosynthetic photon flux density and maximum potential gross photosynthesis. *Photosynthetica*, *48*(4), 596–609. https://doi.org/10.1007/s11099-010-0077-5

Rocky, B. P., & Thompson, A. J. (2018). Production of natural bamboo fibers-1: Experimental approaches to different processes and analyses. *The Journal of The Textile Institute*, *109*(10), 1381–1391. https://doi.org/10.1080/00405000.2018.1482639

Rodtassana, C., Unawong, W., Yaemphum, S., Chanthorn, W., Chawchai, S., Nathalang, A., Brockelman, W. Y., & Tor-ngern, P. (2021). Different responses of soil respiration to environmental factors across forest stages in a Southeast Asian forest. *Ecology and Evolution*, *11*(21), 15430–15443. https://doi.org/10.1002/ece3.8248

Saarela, J. M., Burke, S. V., Wysocki, W. P., Barrett, M. D., Clark, L. G., Craine, J. M., Peterson, P. M., Soreng, R. J., Vorontsova, M. S., & Duvall, M. R. (2018). A 250 plastome phylogeny of the grass family (Poaceae): Topological support under different data partitions. *PeerJ*, *6*, e4299. https://doi.org/10.7717/peerj.4299

Samson, A. O., & Adeniyi, T. A. (2015). Building eco-friendly schools in Ondo state, Nigeria: Focus on the use of bamboo, 11.

Sanchez, L., Mullins, G., Cunningham, J., & Mihelcic, J. (2019). Mechanical properties of bamboo: A research synthesis of strength values and the factors influencing them. *J. Amer. Bamboo Soc.*, *29*, 1–21.

Schmidt, M. W. I., Torn, M. S., Abiven, S., Dittmar, T., Guggenberger, G., Janssens, I. A., Kleber, M., Kögel-Knabner, I., Lehmann, J., Manning, D. A. C., Nannipieri, P., Rasse, D. P., Weiner, S., & Trumbore, S. E. (2011). Persistence of soil organic matter as an ecosystem property. *Nature*, *478*(7367), 49–56. https://doi.org/10.1038/nature10386

Shaikh, J., Yamsani, S. K., Sekharan, S., & Rakesh, R. R. (2019). Performance Evaluation of 5TM Sensor for Real-Time Monitoring of Volumetric Water Content in Landfill Cover

System. *Advances in Civil Engineering Materials*, *8*(1), 20180091. https://doi.org/10.1520/ACEM20180091

Sierra, C. A., Müller, M., & Trumbore, S. E. (2012). *Models of soil organic matter decomposition: The SOILR package, version 1.0* (preprint). Biogeosciences. https://doi.org/10.5194/gmdd-5-993-2012

Singer, A. (2008). Soil horizon designations in the WRB soil classification system. *Encyclopedia of Soil Science* (pp. 668–670). Springer Netherlands.

Six, J., Conant, R. T., Paul, E. A., & Paustian, K. (2002). Stabilization mechanisms of soil organic matter: Implications for C-saturation of soils, 22.

Six, J., Elliott, E., & Paustian, K. (2000). Soil macroaggregate turnover and microaggregate formation: A mechanism for C sequestration under no-tillage agriculture. *Soil Biology and Biochemistry*, *32*(14), 2099–2103. https://doi.org/10.1016/S0038-0717(00)00179-6

Soil Atlas of Europe. (2005). Retrieved June 24, 2022, from https://esdac.jrc.ec.europa.eu/content/soil-atlas-europe

Srivastava, P., Singh, R., Tripathi, S., Singh, H., & Raghubanshi, A. S. (2016). Soil carbon dynamics and climate change: Current agro-environmental perspectives and future dimensions. *Energy, Ecology and Environment*, *1*(5), 315–322. https://doi.org/10.1007/s40974-016-0024-9

Tian, Q., He, H., Cheng, W., Bai, Z., Wang, Y., & Zhang, X. (2016). Factors controlling soil organic carbon stability along a temperate forest altitudinal gradient. *Scientific Reports*, *6*(1), 18783. https://doi.org/10.1038/srep18783

Tiefenbacher, A., Sandén, T., Haslmayr, H.-P., Miloczki, J., Wenzel, W., & Spiegel, H. (2021). Optimizing Carbon Sequestration in Croplands: A Synthesis. *Agronomy*, *11*(5), 882. https://doi.org/10.3390/agronomy11050882

Tomczak, M., & Tomczak, E. (2014). The need to report effect size estimates revisited. An overview of some recommended measures of effect size. *1*, 7.

Tsui, C.-C., Tsai, C.-C., & Chen, Z.-S. (2013). Soil organic carbon stocks in relation to elevation gradients in volcanic ash soils of Taiwan. *Geoderma*, *209-210*, 119–127. https://doi.org/10.1016/j.geoderma.2013.06.013

UC San Diego. (2022). Retrieved July 1, 2022, from https://keelingcurve.ucsd.edu/

United Nations. (2021). Retrieved June 20, 2022, from https://www.un.org/en/climatechange/cop26

Van Ranst, E., & Sys, C. (2000). *Eenduidige legende voor de digitale bodemkaart van Vlaanderen (schaal 1:20 000)*. Universiteit Gent.

Virto, I., Barré, P., Burlot, A., & Chenu, C. (2012). Carbon input differences as the main factor explaining the variability in soil organic C storage in no-tilled compared to inversion

tilled agrosystems. *Biogeochemistry*, *108*(1-3), 17–26. https://doi.org/10.1007/s10533-011-9600-4

Viscarra Rossel, R. A., Webster, R., Bui, E. N., & Baldock, J. A. (2014). Baseline map of organic carbon in Australian soil to support national carbon accounting and monitoring under climate change. *Global Change Biology*, *20*(9), 2953–2970. https://doi.org/10.1111/gcb.12569

Wesselingh, F., & van den Hoek, L. (n.d.). Geologie Van Nederland. Retrieved June 28, 2022, from https://www.geologievannederland.nl/tijd/reconstructies-tijdvakken/vroeg-pleistoceen

West, T. O., & Six, J. (2007). Considering the influence of sequestration duration and carbon saturation on estimates of soil carbon capacity. *Climatic Change*, *80*(1-2), 25–41. https://doi.org/10.1007/s10584-006-9173-8

Wiesmeier, M., Urbanski, L., Hobley, E., Lang, B., von Lützow, M., Marin-Spiotta, E., van Wesemael, B., Rabot, E., Ließ, M., Garcia-Franco, N., Wollschläger, U., Vogel, H.-J., & Kögel-Knabner, I. (2019). Soil organic carbon storage as a key function of soils - A review of drivers and indicators at various scales. *Geoderma*, *333*, 149–162. https://doi.org/10.1016/j.geoderma.2018.07.026

Yang, X.-D., Ali, A., Xu, Y.-L., Jiang, L.-M., & Lv, G.-H. (2019). Soil moisture and salinity as main drivers of soil respiration across natural xeromorphic vegetation and agricultural lands in an arid desert region. *CATENA*, *177*, 126–133. https://doi.org/10.1016/j.catena.2019.02.015

Yoro, K. O., & Daramola, M. O. (2020). CO2 emission sources, greenhouse gases, and the global warming effect. *Advances in Carbon Capture* (pp. 3–28). Elsevier. https://doi.org/10.1016/B978-0-12-819657-1.00001-3

Yuan, W., Luo, Y., Liang, S., Yu, G., Niu, S., Stoy, P., Chen, J., Desai, A. R., Lindroth, A., Gough, C. M., Ceulemans, R., Arain, A., Bernhofer, C., Cook, B., Cook, D. R., Dragoni, D., Gielen, B., Janssens, I. A., Longdoz, B., ... Varner, R. (2011). Thermal adaptation of net ecosystem exchange. *Biogeosciences*, *8*(6), 1453–1463. https://doi.org/10.5194/bg-8-1453-2011

Yuen, J. Q., Fung, T., & Ziegler, A. D. (2017). Carbon stocks in bamboo ecosystems worldwide: Estimates and uncertainties. *Forest Ecology and Management*, *393*, 113–138. https://doi.org/10.1016/j.foreco.2017.01.017

Zhang, Y.-X., Guo, C., & Li, D.-Z. (2020). A new subtribal classification of Arundinarieae (Poaceae, Bambusoideae) with the description of a new genus. *Plant Diversity*, *42*(3), 127–134. https://doi.org/10.1016/j.pld.2020.03.004

Zhou, G., Meng, C., Jiang, P., & Xu, Q. (2011). Review of Carbon Fixation in Bamboo Forests in China. *The Botanical Review*, *77*(3), 262–270. https://doi.org/10.1007/s12229-011-9082-z

Zhou, Z., Guo, C., & Meng, H. (2013). Temperature Sensitivity and Basal Rate of Soil Respiration and Their Determinants in Temperate Forests of North China (D. Hui, Ed.). *PLoS ONE*, *8*(12), e81793. https://doi.org/10.1371/journal.pone.0081793

Appendix A
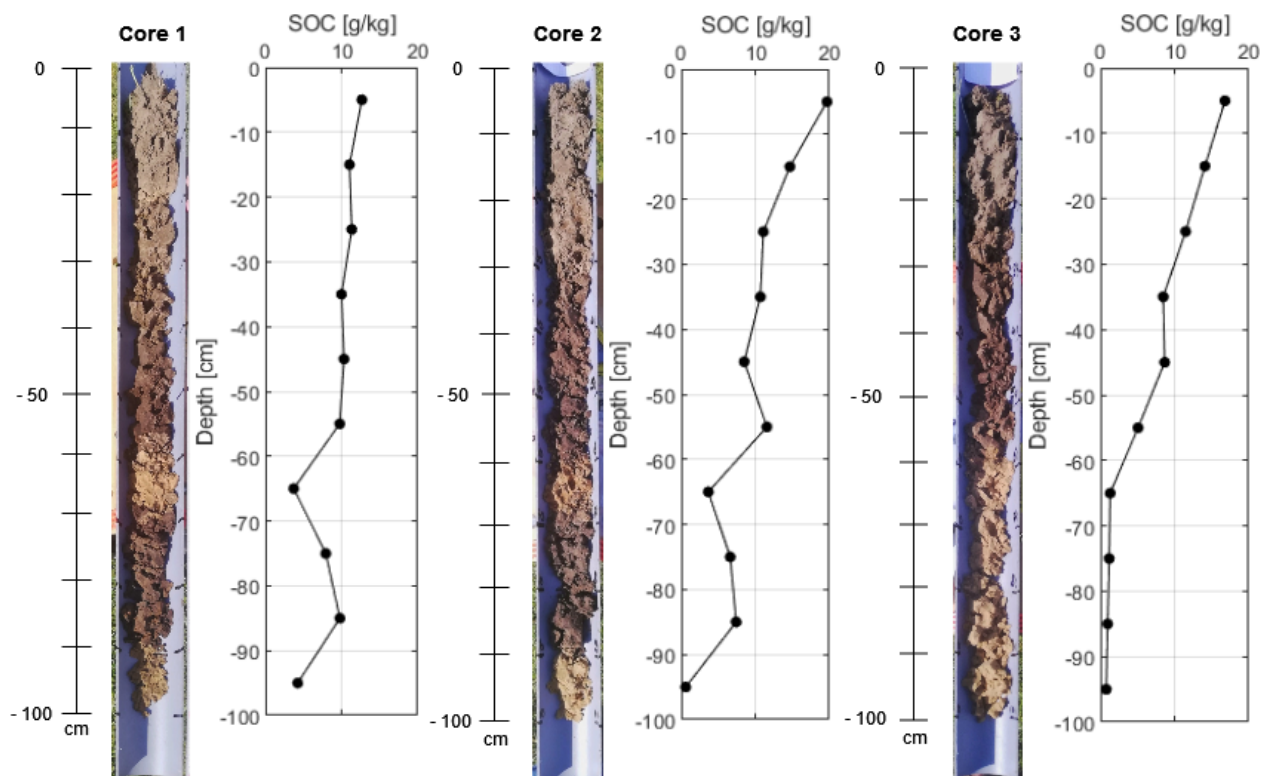
A.1 Vertical distribution of SOC in the grassland

Figure A.1: Vertical distribution of SOC [gC/kg] for each of the first three auger samplings (prospecting) in the grassland. The contents were obtained by dry combustion. The values in the graph can be visually correlated to the soil profile at the same level. Each black dot represents a measured value.

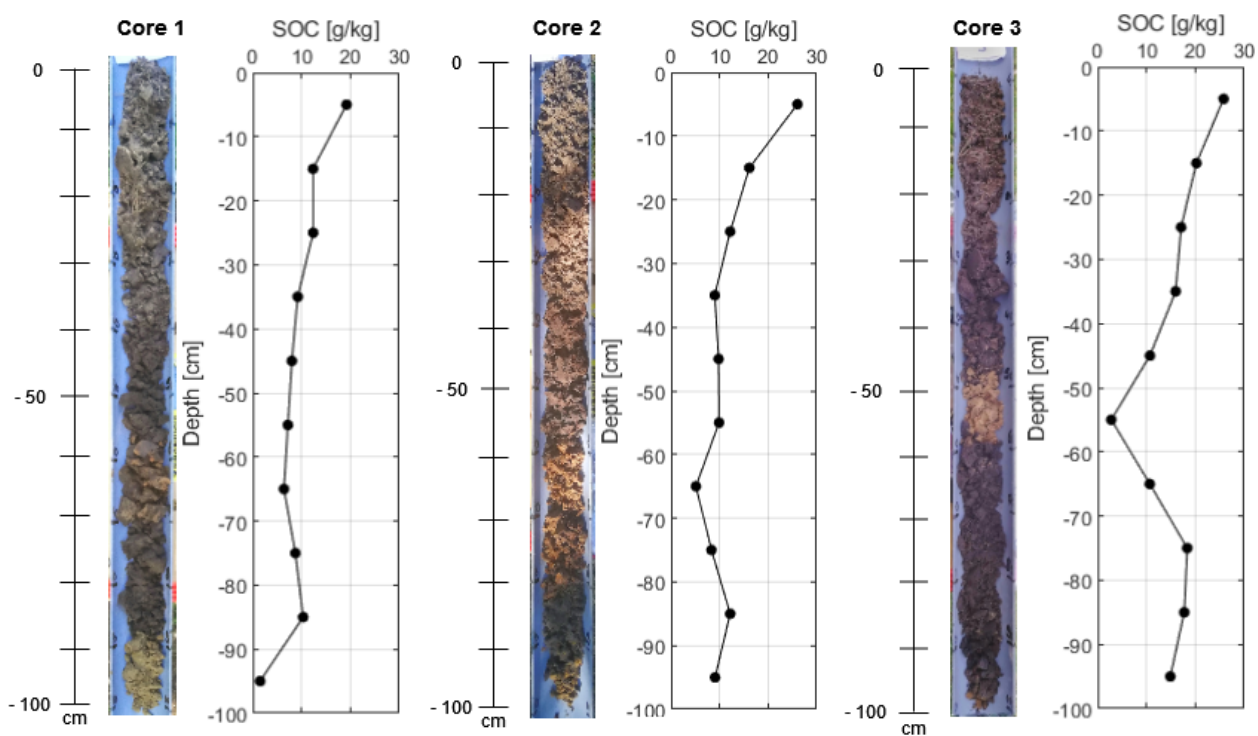## A.2 Vertical distribution of SOC in the black bamboo

Figure A.2: Vertical distribution of SOC [gC/kg] for each of the first three auger samplings (prospecting) in the black bamboo (*Phyllostachys nigra*). The contents were obtained by dry combustion. The values in the graph can be visually correlated to the soil profile at the same level. Each black dot represents a measured value.

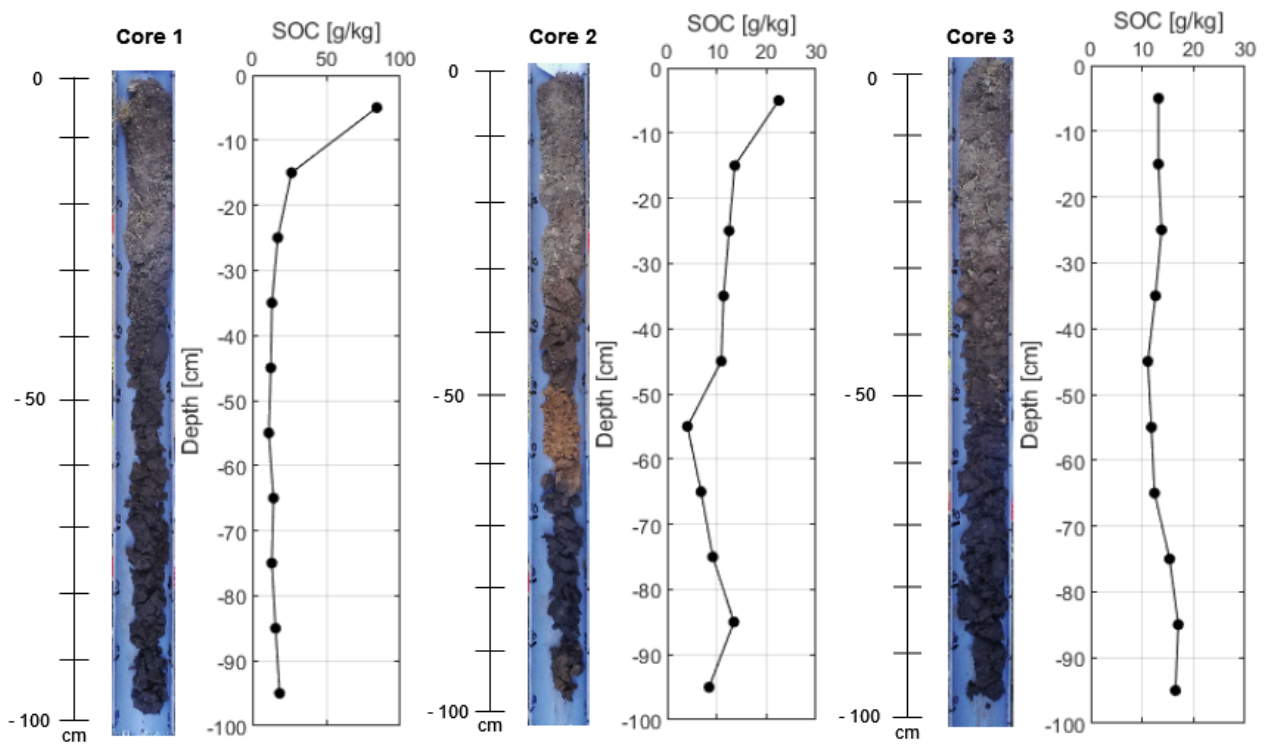## A.3   Vertical distribution of SOC in the green bamboo

Figure A.3: Vertical distribution of SOC [gC/kg] for each of the first three auger samplings (prospecting) in the green bamboo (*Phyllostachys aurea*). The contents were obtained by dry combustion. The values in the graph can be visually correlated to the soil profile at the same level. Each black dot represents a measured value. *The horizontal axis scales are different.*

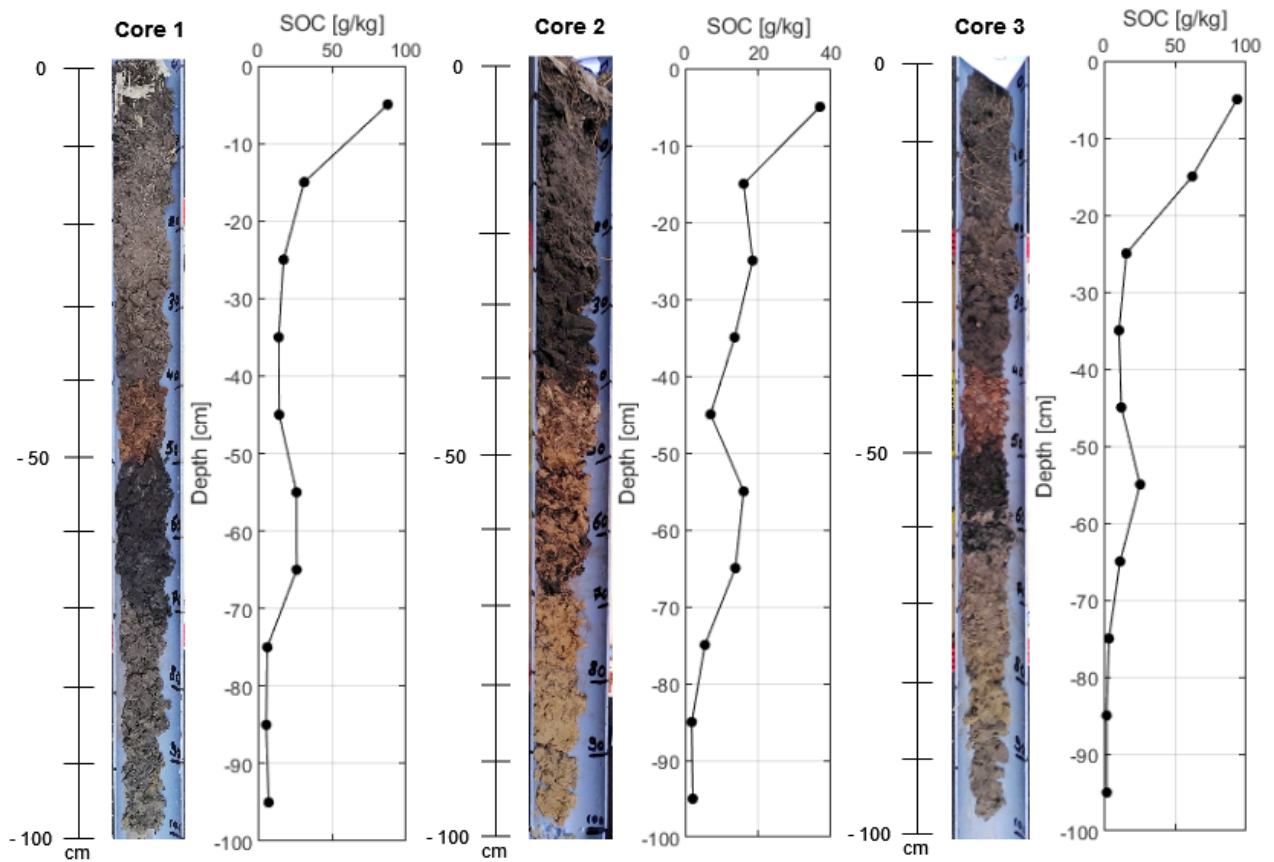# A.4 Vertical distribution of SOC in the yellow bamboo

Figure A.4: Vertical distribution of SOC [gC/kg] for each of the first three auger samplings (prospecting) in the yellow bamboo (*Phyllostachys aureosulcata*). The contents were obtained by dry combustion. The values in the graph can be visually correlated to the soil profile at the same level. Each black dot represents a measured value. *The horizontal axis scales are different.*

Appendix B

B.1 Soil respiration measurement metadata

Table B.1: Environmental parameters from CO_2 efflux measurements. The climatic data are taken from the weather station in Retie, the closest to Merksplas.

Date	Start	End	Air Temperature [°C]	Air humidity [%]	Rain [mm]
April 6	9:30 am	3:00 pm	10	$75-83$	$0-2$
April 22	1:00 pm	4:00 pm	15	57	0
May 3	9:30 am	3:00 pm	$14-17$	$46-53$	0
May 21	10:30 am	3:00 pm	19	$52-61$	0
June 5	11:00 am	3:00 pm	17	$92-98$	15
June 22	9:00 am	3:00 pm	$20-25$	$59-39$	0